CHALMERS UNIVERSITY OF TECHNOLOGY

MASTER'S THESIS (30 HP)

DEPARTMENT OF BIOLOGY AND BIOLOGICAL ENGINEERING

AUGUST 2021 - JANUARY 2022

Influence of ethanol on xylose metabolism in engineered *S. cerevisiae* and applicability in continuous ethanol production

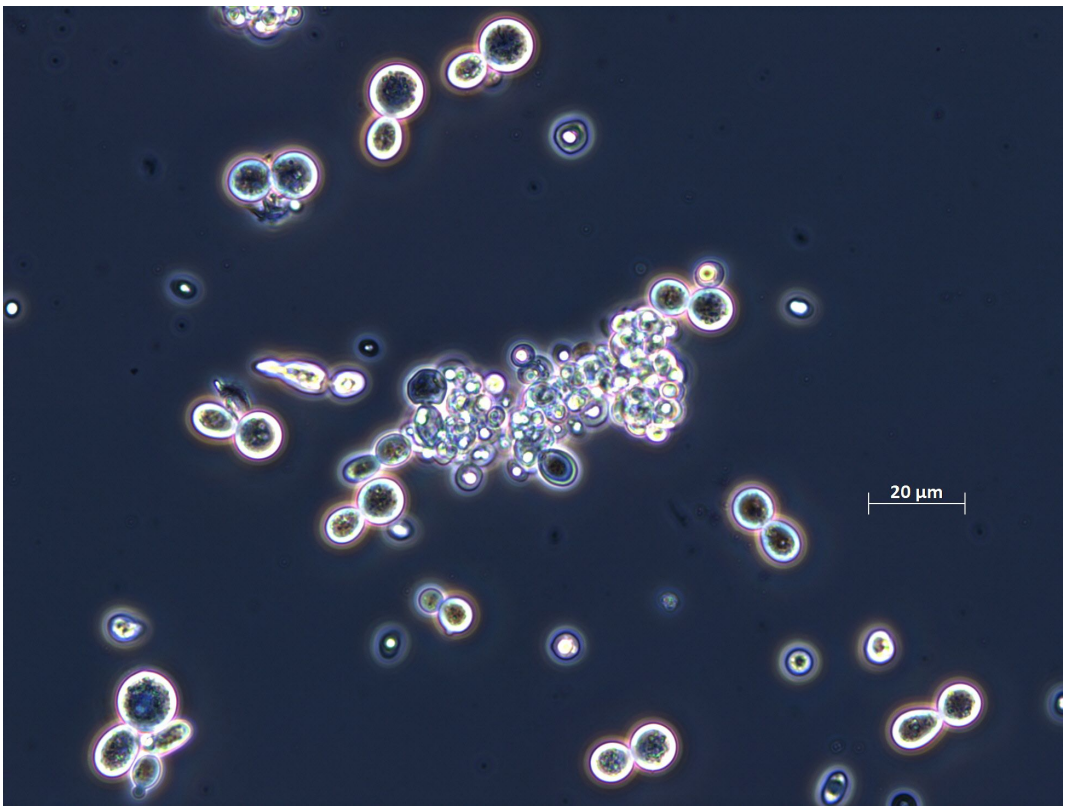

Author:
MATHILDA JOHANSSON
Examiner:
CARL JOHAN FRANZÉN, CHALMERS UNIVERSITY OF TECHNOLOGY
Supervisor:
ADNAN CAVKA, SEKAB

Preface

This study was performed in collaboration with and financed by Sekab E-Technology AB in Örnsköldsvik, Sweden. Laboratory facilities and equipment were provided by MoRe Research, Örnsköldsvik. The project was supervised by Dr. Adnan Cavka (Sekab) and examinor of the master thesis was Professor Carl Johan Franzén (Institute of biology and biological engineering, Chalmers University of Technology).

Abstract

There is a rapidly growing market for renewable substitutes to fossil-based fuels and chemicals due to increased awareness of global warming and political efforts to reduce emissions. Sekab E-technology AB develops and licenses technologies for bioethanol production from forest residues, converting various sugar types found in cellulose and hemicellulose into ethanol using the yeast *Saccharomyces cerevisiae*. Beyond their native pathways for utilization of glucose and other hexose monomers, strains used at Sekab have been engineered with a pathway for xylose metabolism.

Co-fermentation of glucose and xylose results in a higher yield of ethanol, but productivity is exceedingly reduced if xylose fermentation is allowed to proceed until depletion. Extensive attempts to increase flux through the xylose pathway using metabolic engineering have been reported, but investigations of the impact of process-related parameters on co-fermentation are scarce. At Sekab, recent experiments have indicated that externally added ethanol may have a different effect on the fermentative rate of xylose compared to glucose in co-fermenting cultures on hydrolysate. This thesis aimed towards further investigating how external addition of ethanol influences the rate of fermentation in glucose and xylose co-fermenting batch cultures in defined media. In the present study, the fermentation rate decreased by 22 $\%$ during glucose consumption and increased by 25 $\%$ during xylose consumption when 20 gL^{-1} ethanol was added to co-fermenting cultures. Maximum xylose consumption rate appeared independent of both glucose concentration and ethanol addition, although the timing of xylose consumption onset was highly dependent on both. No difference in allocation of carbon between growth and ethanol formation was observed. As such, the effect of ethanol could not be attributed to prolonged glucose availability nor to increased growth during the glucose consuming phase.

Co-fermenting batch cultures were also simulated computationally based on a combination of previously suggested kinetic models. A comparison of model-predicted behaviour with experimental data indicated that glucose kinetics cannot describe all aspects of xylose metabolism, in particular when glucose levels are low. Nevertheless, Sekab's continuous fermentation regime was simulated using the existing models. While further modification of the model is needed for accurate representation of co-fermentation, feed-rate control based on measurements of refractive index (RI) appeared to be an efficient control system for continuous fermentation. The simulation also constituted a proof-of-concept that, when further developed, will provide demonstrative value for costumer-adapted *in silico* test runs. Overall, results presented in this report highlight the lack of knowledge about glucose and xylose co-fermentation dynamics and the need for further research.

Keywords: Sustainable, fermentation, ethanol, yeast, S. cerevisiae, hydrolysate, xylose

Contents

List of Figures

List of Tables

1 Introduction

During the past century, emissions of greenhouse gases (GHGs) have increased globally at an alarming rate. In particular, the level of carbon dioxide in the atmosphere has increased drastically, from 315 ppm in 1958 to the current level of 414 ppm (2021) [1]. As reported by the Intergovernmental Panel on Climate Change (IPCC) [2], GHGs impact both human and natural systems in every continent and across biomes by interfering with the climate system. Projected risks for humanity include scarcity of fresh water and food access, more frequent and severe occurrences of extreme weather, displacement of populations, irreversible regime shifts in ecosystems and floodings of entire areas due to rising sea levels. To mitigate such catastrophic effects, a combination of actions towards climate adaptation and an abrupt reduction of carbon release into the atmosphere are necessary.

Carbon dioxide is released by humans and other heterotrophs as part of their central metabolism, as well as in several other natural biological processes. However, the main contributor towards increasing levels of carbon dioxide is global combustion of fossil fuels. The main source of emissions is the global energy sector, representing 73.2 % of global GHG emissions [3] (Figure 1). Within this sector, energy use in industry, buildings and transportation account for the majority [3].

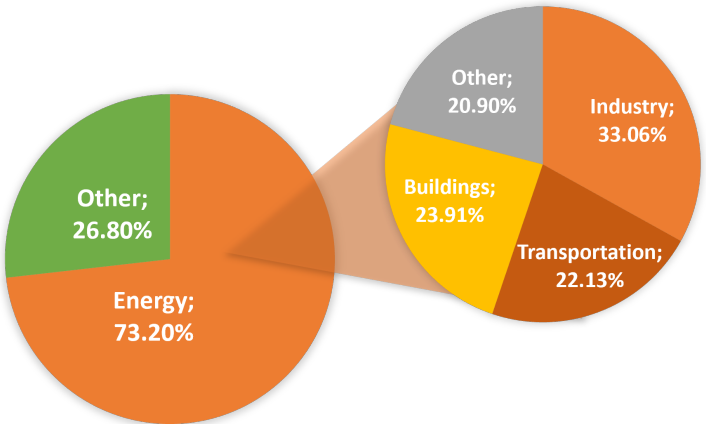

Figure 1: Emission of greenhouse gases globally by sector. Data adapted from *Our world in data: CO_2 and Greenhouse Gas Emissions* [3].

In order to reduce emissions from the transportation sector, the Swedish government introduced the Swedish greenhouse gas reduction mandate in 2018. With obligations on fuel producers to reduce their fossil emissions by a certain fraction each year (Figure 2), the goal of the mandate is to contribute towards achieving a 70 % reduction of GHG emissions by 2030 compared to 2010 [4]. This will inevitably generate a rapidly increasing demand for, among others, gasoline miscible biofuels such as ethanol.

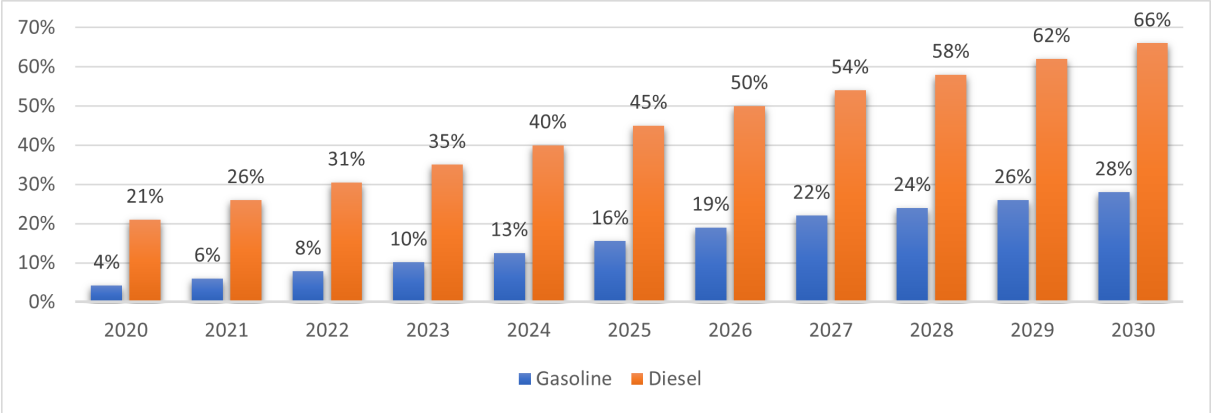

Figure 2: Yearly requirement of greenhouse gas emission reduction according to the Swedish greenhouse gas reduction mandate. Data adapted from SFS 2021 [5].

By definition, biofuels are "any fuel that is derived from biomass" [6]. When bio-based ethanol blended with gasoline was first introduced when prices on oil went up in the 1920s, the predominant source of biomass was corn. However, as the issue of competition with food supply emerged, biofuels based on forest and agricultural residues eventually became more widely used and are today referred to as 2^{nd} generation biofuels [7]. Sweden holds great potential for this type of fuels, being the world's 5^{th} largest exporter of pulp, paper and timber [8]. Furthermore, almost 70 $\%$ of the Swedish land area is covered in forest [9] and the amount of forest biomass has been steadily increasing during the past century, despite an expanding forest industry [10]. In Örnsköldsvik, ethanol production dates all the way back to 1909 and has since then characterized the area and promoted infrastructural development. Today, lignocellulose from wood is refined into everything from chemicals like ethanol and acetaldehyde to paper and textiles. Sekab (Svensk Etanol Kemi AB) was founded by actors within this sector in 1985 and soon thereafter became the first ethanol fuel producer for buses (E85) in Europe. Starting in 1997, Sekab split into Sekab Chemicals and Biofuels and Sekab E-Technology AB. The aim of the latter was to develop a forest-based ethanol production pilot plant, and since its foundation Sekab E-Technology AB has licensed several advanced technical solutions for lignocellulosic bioethanol production [11].

Lignocellulose is the main component in wood and consists predominantly of cellulose, hemicellulose and lignin. Cellulose consists of glucose monomers linked in a strictly organized way, providing strength and stability to the wood structure. Hemicellulose is composed of a mix of different sugar monomers including xylose, mannose, arabinose and galactose. These are arranged in a branched network that stretches around the cellulose fibers. Finally, lignin is a complex polymer of interconnected aromatic rings, making the cellulose resistant to enzymatic degradation. Ethanol is produced through fermentation of the various sugar types found in cellulose and hemicellulose. The sugar composition largely depends on the tree species (Table 1), as well as other properties such as the age of the tree. Glucose is the dominant sugar monomer in all wood species as it constitutes the building block of cellulose, while the others are present in various degrees. Softwood typically has higher galactose, mannose and arabinose content, while xylose is present in larger amounts in hardwood. The ratio between cellulose, hemicellulose and lignin also varies between wood species [12].

Wood species	Glucose	Galactose	Mannose	Xylose	Arabinose
Hardwood (%)	39-52	0-2	1.8-3.6	15-26	0.3-0.8
Softwood (%)	42-46	1-4.7	7.4-12	2.8-10	0.5-2.7

Table 1: Percent of sugar monomers in oven-dry wood from hardwood versus softwood. Data adapted from RC Pettersen 1984 [12, page 115-116].

Bioethanol is commonly produced through fermentation by the yeast *Saccharomyces cerevisiae*, which converts several sugar types into ethanol with high productivity [13]. Due to the complex structure of lignocellulose described above, wood must however be processed prior to fermentation to make the sugar accessible. Consequently, bioethanol production form lignocellulose requires at least four key process steps; pretreatment, enzmatic hydrolysis, fermentation and distillation [14]. Although there are several different methods available for each step [15], only the specific methods implemented in Sekab's process are described below (Figure 3) [16]. During pre-treatment, sulphuric acid or sulphur dioxide and steam at 170-200 °C are added, breaking the cellulose and hemicellulose structures through a process called steam explosion. Next, enzymes are added to hydrolyze the cellulose and hemicellulose into their sugar constituents. Fermentation can either be performed after hydrolysis (Separate hydrolysis and fermentation, SHF) or simultaneously with hydrolysis (Simultaneous sacchrification and fermentation, SSF). Either way, yeast is added to convert sugar into ethanol and carbon dioxide. After fermentation, yeast cells are separated from the liquid and a fraction is recirculated back to the fermentation tank. Finally, ethanol is separated from fermentation byproducts and water through distillation. Lignin is separated in a centrifuge either before fermentation or after distillation and can be used in other applications [16].

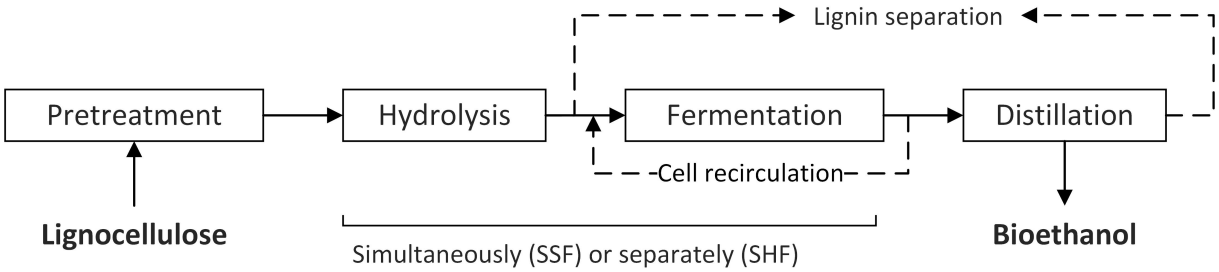

Figure 3: Process steps in the conversion of lignocellulose into pure ethanol. Hydrolysis and fermentation can be performed separately or simultaneously, and lignin is separated from the media either before fermentation or after distillation. A fraction of cells are recirculated back to the fermentation tank.

Fermentation using either SHF or SSF may advantageously be performed in continuous mode, yielding a higher volumetric productivity, less use of chemicals, a superior process stability and reduced requirement of microbe propagation [17] [18]. However, continuous fermentation comes with a number of challenges constraining ethanol yield and productivity metrics in the long run. Firstly, imperfect sterilization procedures and abundantly available sugars render a high risk of contamination [18], resulting in lower yields as sugar is consumed by non-ethanol producing contaminants. Secondly, maintaining a stable process requires that the flow rate is controlled so that an optimal amount of sugar is fed in proportion to the amount of yeast being washed out. Due to occasionally large fluctuations of sugar composition and concentrations in the feed, the optimal

flow rate changes over time, putting demands on online measurements as input for flow rate control. Another parameter that must be controlled is the proportion of cells to be recirculated back into the tank. Finally, yeasts prefer some sugar types over others and some are therefore consumed earlier and faster. This results in a trade-off where a faster flow rate renders higher productivity but lower yield due to incomplete fermentation of some sugar types. Xylose is a typical example of this effect, being fermented after glucose exhaustion and at a lower rate [19].

In the current process at Sekab, xylose is usually not fully fermented as productivity is prioritized at the expense of final yield. However, recent and not yet published research at Sekab has showed that ethanol can have a positive effect on fermentation rate during the latter phase of fermentation, when pentoses such as xylose are fermented. While ethanol-spiked microbial cultures grow and ferment at lower rates during the glucose-consuming phase, they appear to gradually catch up with cultures without ethanol during the latter phase of fermentation. This effect was demonstrated both in lab-scale batch cultures and pilot scale continuous fermentations, and has the potential of yielding an increased ethanol productivity during pentose consumption. However, neither the biological mechanisms responsible nor the specific conditions required for the phenomenon to occur have been identified. As such, further investigation of the effect is crucial for practical implementation.

1.1 Scope

The primary question investigated in this study was why fermentative rate increases during the latter phase of glucose and xylose co-fermenting batch cultures when moderate levels of ethanol are added. For this purpose, the following research questions were addressed:

1. Can the effect of ethanol on fermentative rate of xylose be demonstrated in defined media?
2. Is the presence of glucose a decisive factor for fermentative rate of xylose?
3. If glucose presence is not a decisive factor, what other factors may have a significant impact?
4. Can the observed effect be used to increase ethanol productivity during xylose fermentation in a continuous fermentation regime?

The purpose of question (1) was to determine whether the effect is an intrinsic property of yeast occurring due to mechanisms in its generic metabolism, or if it is due to the specific environment created in lignocellulose-based ethanol production. If the effect can be demonstrated in defined media, numerous possible causing agents such as inhibitory compounds and other by-products of lignocellulosic processing can be ruled out. Question (2) addresses a first hypothesis about why this effect occurs. As will be described in greater detail, glucose influences xylose uptake and could be a mediating component of the impact of ethanol on xylose fermentation. The third question allows for discussion of alternative hypotheses to be investigated, possibly addressing xylose concentration, biomass concentration and timing of ethanol addition. Finally, building on the results of previous questions, the fourth question addresses how results from this study can provide value for industrial scale fermentations.

1.2 Aim

The aim of this thesis was to evaluate how externally added ethanol influence the rate of xylose consumption, ethanol formation and growth of *Saccharomyces cerevisiae* during glucose and xylose co-fermentation.

1.3 Limitations

In order to isolate fundamental cellular mechanisms related to xylose fermentation in presence of ethanol, the scope of this project was limited in several aspects. Firstly, the molecular complexity of lignocellulosic hydrolysates renders a diverse environment for studies of fermentation. To reduce the number of variables that potentially influence rates of growth and fermentation, a defined media with only essential substrates was used throughout the investigation. As such, the impact of inhibitory compounds, acids of various types and sugar monomers beyond glucose and xylose were not addressed. Secondly, ethanol can be produced using a range of different microbial factories, including fungi, bacteria and algae. However, various strains of *S. cerevisiae* are commonly preferred due to their many favorable traits. Several such strains have been evaluated at Sekab, but the continuous fermentation technology has been shown to be strain independent. For the scope of this project, one commercially available xylose-fermenting strain was chosen, excluding any other microbial factories. Lastly, results deemed useful from this study will be implemented in Sekab's continuous fermentation technology, but experimental work was performed in small scale batch cultures due to technical constraints and for sake of simplicity. Effects in continuous fermentation regimes were only investigated through computational modelling.

2 Background

Behind the conversion of sugar into ethanol lie complex biological mechanisms developed through millions of years of evolution. Optimizing and controlling industrial fermentation processes can be greatly facilitated by understanding mechanisms on microscopical level such as metabolic pathways and their regulation. This section addresses relevant concepts of carbon metabolism in yeast, metabolic engineering behind xylose utilization and regulatory mechanisms coordinating carbon utilization. Previously suggested kinetic models of glucose and xylose co-fermentation are subsequently reviewed, and finally the technical design of a continuous fermentation process developed and demonstrated in the Biorefinery Demo Plant in Örnsköldsvik is described.

2.1 Carbon metabolism

Carbon consumed by cells can be allocated towards different end products depending on environmental circumstances. Energy is needed for survival and growth, and can be obtained through respiration, fermentation, or a combination thereof. In anaerobic conditions, fermentation is the preferred option for energy generation. However, in aerobic conditions cells can moderate their metabolism between various activities, among them respiration and fermentation. Energy-wise it is preferable for the cell to perform respiration, yielding approximately 18 ATP units in contrast to 2 ATP units during fermentation in *S.cerevisiae* [20]. Nevertheless, *S. cerevisiae* display diauxic growth in aerobic batch cultures where fermentation is preferred during the initial phase, followed by respiration towards the latter phase [21, Chapter 2]. This is known as the Crabtree effect: yeasts prefer fermentation over respiration at high glucose levels despite a reduced yield of energy [22]. Pfeiffer and Morley 2014 [20] review two theories attempting to explain the Crabtree effect from an evolutionary perspective; the make-accumulate-consume strategy (MAC) and the rate/yield trade-off hypothesis (RYT). MAC suggests that aerobic fermentation provides a competitive advantage as ethanol is toxic to most organisms and cannot be consumed by most other microorganisms. The RYT theory suggests that, when it comes to ATP, productivity constitutes a stronger incentive than yield. Thus, while aerobic fermentation is less efficient than respiration, ATP is produced faster providing an advantage for the yeast [20]. The actual evolutionary cause of the Crabtree effect is a controversial subject, but as pointed out by the authors, both RYT and MAC provide incentives to perform fermentation aerobically. When glucose is less abundant, it makes more sense for the cells to maintain a high yield of ATP per glucose unit, suggesting an explanation to why respiration kicks in.

2.2 Xylose assimilating pathways

Wild-type *S. cerevisiae* holds endogenous genetic sequences for xylose assimilation, theoretically enabling an oxidoreductive xylose utilization pathway. However, flux through this pathway does not occur at measurable levels [23]. Instead, *S. cerevisiae* strains used in industrial fermentation processes have been engineered with exogenous pathways from microorganisms including *Pichia stipitis* [24] and *Piromyces* [25]. Such pathways allow for the conversion of xylose into D-xylulose-5P, which can enter the pentose phosphate pathway (PPP) (Figure 4). These fungi employ different strategies for assimilating xylose, the former using a xylose reductase (XR) and

xylitol dehydrogenase (XDH) and the latter using a xylose isomerase (XI). XR converts xylose into D-xylitol, which is converted into D-xylulose by XDH. XI circumvents the xylitol step by directly converting xylose into D-xylulose. In both pathways, D-xylulose is subsequently phosphorylated into D-xylulose-5-P by the endogeneous enzyme xylulose kinase (XK) [26].

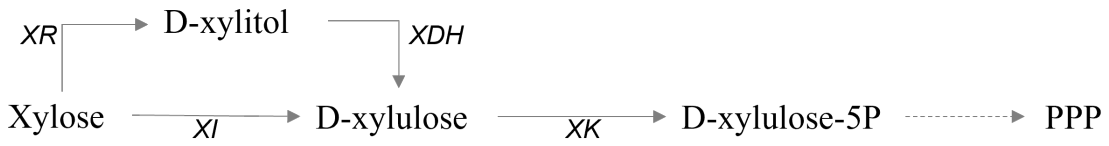

Figure 4: Schematic illustration of two metabolic pathways for xylose that have been introduced in *S. cerevisiae*. XR: xylose reductase, XDH: Xylitol dehydrogenase, XI: xylose isomerase, XK: xylulose kinase. PPP: Pentose Phosphate Pathway.

Despite extensive attempts using metabolic engineering, engineered strains consume xylose at significantly lower rates than glucose. Two possible explanations to slow xylose consumption dominate in previous reports. The first addresses effects on the redox balance of the cell, impacted by xylose fermentation as both enzymes in the *P. stipitis* pathway are cofactor dependent. XR utilizes primarily NADPH (although NADH can be used as well but at a lower affinity) [27], a cofactor produced in the PPP that plays a key role in biosynthetic pathways. XDH uses NAD+ when catalyzing the conversion of D-xylitol into D-xylulose. As *S. cerevisiae* lacks the enzyme to transfer protons between NADH and NADPH [28], xylose metabolism becomes a redox imbalanced reaction requiring regeneration of both NADPH and NAD+ through other pathways. This imbalance results in secretion of excess xylitol and a reduced yield of ethanol. The XI pathway, on the other hand, is not subject to this explanation as it is co-factor independent.

Xylose uptake is generally considered the rate limiting step in xylose metabolism [29] and constitutes another explanation to slow xylose metabolism. The group of proteins involved in sugar uptake include 17 hexose permeases (hxt) that allow for transportation of D-glucose, D-mannose and D-fructose across the cell wall using facilitated diffusion. There is also gal2, a transporter specific for galactose, and two glucose sensing proteins, snf3 and rgt2 [30]. Uptake of pentoses through hxt proteins occurs, but their overall affinity for xylose is very low compared to glucose. Attempts have therefore been made to introduce other pentose transport systems using metabolic engineering [31], but unfortunately the proteins constituting the highly efficient pentose transport system in *P. stipitis* have not yet been identified and isolated [27]. Attempts to increase xylose uptake by introducing a transporter protein from *Candida intermedia* have been made [32], but to the author's knowledge there is still no commercial strain in which an exogenous xylose transport system has been successfully demonstrated.

2.3 Regulatory mechanisms

Beyond the issue of glucose preference in native sugar transport proteins, efficient xylose fermentation is likely limited by complex regulatory mechanisms. These have been developed throughout evolution and optimized for the sugar monomers most commonly consumed. Consequently, cells display a dynamic transcriptional behaviour in response to changing extracellular sugar concentrations. For example, a comparison of transcription profiles between *S. cerevisiae* expressing

the XR/XDH pathway from *P. stipitis* growing on glucose versus xylose revealed that genes related to NADH regeneration were upregulated in xylose cultures, as well as some genes related to glucose starvation [33]. The same research group later observed reduced expression levels of central metabolic pathways including the glyoxylate cycle, TCA cycle and respiratory genes, but increased abundance of glycolytic enzymes [34].

Responses to extracellular and intracellular glucose levels are coordinated by two glucose-sensing proteins, snf3 and rgt2 [35]. These are structurally similar to hexose transporters but incapable of performing sugar transportation themselves. Snf3 is activated when glucose approaches exhaustion, promoting the expression of high affinity hexose transporters and allowing for genes involved in alternative carbon source utilization to be expressed. When glucose is abundant, Snf3 is inactive and prevents utilization of alternative carbon sources. High levels of glucose also activates rgt2, promoting expression of low affinity hexose transporters. When glucose is absent, neither rgt2 nor snf3 are active and both high and low affinity transporters are repressed [35]. Notably, there has been some evidence that snf3 induce expression of some *HXT* genes in the presence of xylose and that xylose can alter the conformation of both rgt2 and snf3 [36].

Saloheimo et al. 2007 [31] found that a *S. cerevisiae* strain with *HXT1-HXT7* and *GAL2* deletions (*hxt null*), expressing only one of *HXT1*, *HXT2*, *HXT4*, *HXT7* or *GAL2* individually, could grow on xylose but observed an extended lag phase (five to ten days depending on which transporter was used) for all cultures except the *GAL2* strain. The lag phase was shortest in the strain expressing *HXT1*, followed by *HXT7*. Further investigation of the same transporters was performed by Goncalves et al. 2014 [29] who analyzed the impact of individual hexose transporters on xylose fermentation instead of growth. The *hxt null* strain expressing *HXT1* did not ferment xylose at significant rates when given as sole carbon source, but allowed for maximum ethanol production during co-fermentation with glucose. This observation is in agreement with the regulations described in Table 2, suggesting that glucose is required to induce the expression of *HXT1*. However, Goncalves et al. 2014 ended the fermentations after approximately 80 hours. At this point, only approximately 50 % of the added xylose had been consumed in the co-fermenting culture. Furthermore, with xylose as sole carbon source, 80 hours is too short for the delayed initiation of xylose consumption observed by Saloheimo et al. 2007 to occur. Table 2 summarizes the affinity and regulation of each hxt protein according to Horak 2013 [30].

Gene	**Glucose affinity**	**Regulation**
HXT1	Low	Induced by high concentrations of glucose.
HXT2	Moderate	Induced by low concentrations of glucose
HXT3	Low	Weakly dependent on glucose concentration.
HXT4	Moderate	Induced by low concentration of glucose.
HXT5	Moderate	Regulated by growth rate (Maximum uptake at slow growth)
HXT6	High	Induced by low concentration of glucose
HXT7	High	Induced by low concentration of glucose
HXT8-17	-	Poorly defined, normally silent

Table 2: Summary of hexose transporter glucose affinity and regulation, all data adapted from Horak 2013 [30].

2.4 Modelling co-fermentation

Biological reactions are often described through Michaelis Menten (MM) kinetics, relating reaction rate *v* with substrate concentration *[S]* based on a maximum reaction rate V_{max} and a substrate saturation constant K_m. MM kinetics are defined based on two fundamental assumptions: the steady state approximation (as suggested by Briggs and Haldane [37]) and the free ligand approximation [38]. In the steady-state approximation, the concentration of substrate-enzyme complex and the concentration of free enzymes are assumed to be constant. The free ligand approximation states that the concentration of free substrate is much higher than the concentration of enzyme-bound substrate, implying that the rate of the backwards reaction from substrate-enzyme complex to free substrate and enzyme is negligible in relation to the rate of product formation from the substrate-enzyme complex [38]. As such, the general MM equation assumes that the reaction rate is dependent exclusively on substrate concentration and that reactions are irreversible.

In order to describe the effects investigated in this project, additional dependencies representing substrate and product inhibition must be added to each kinetic expression. As reviewed by Nosrate-Ghods et al. 2020 [39], numerous modifications of the Michaelis Menten equation have been proposed to describe the inhibitory effect of ethanol on growth and the competitive inhibition of glucose on xylose uptake. Levenspiel et al. 1980 [40] proposed an equation for ethanol inhibition on cell growth describing a parabolic relationship between ethanol and growth inhibition, according to equation (1). The equation was validated by Luong et al 1985 [41], who further showed that it is also representative for ethanol inhibition on fermentation. While several other dependencies (linear, exponential and hyperbolic) were considered, they concluded that the parabolic equation can represent any of the mentioned dependencies by changing the value of *a*.

$$v = vmax * \left(1 - \frac{E}{E_{max}}\right)^{a} * \frac{S}{K_s + S} \tag{1}$$

The impact of glucose on xylose uptake constitutes a more complex dependence. One mathematical representation has been proposed in a report by Taumala et al. 2016 [42], in which xylose consumption is inhibited by high levels of glucose through an inhibition constant (K_{glu}). Low levels of glucose instead cause a phase shift, resulting in a reduced yield of ethanol on xylose (equations (2)-(4)). The proposed model further includes an expression representing the lag phase of a culture, the length of which is determined by an empirical constant *tau*. In the article by Taumala et al, equation (4) was used to describe the formation of biomass and several byproducts such as glycerol and acetate. The formation of ethanol and carbon dioxide, however, were determined using a flux balance analysis (FBA).

$$q_{glu} = -vmax1 * \frac{glu}{K1 + glu} * \left(1 - e^{\frac{-t}{tau}}\right) \tag{2}$$

$$q_{xyl} = vmax2 * \frac{xyl}{K2 * (1 + \frac{glu}{K_{glu}})} * \left(1 - e^{\frac{-t}{tau}}\right) \tag{3}$$

$$q_p = -(q_{glu} + q_{xyl}) * Y_{ps} \tag{4}$$

$$Yps = \begin{cases} Yps1 & \text{if } glu > alpha \\ Yps2, & \text{if } glu \leq alpha \end{cases}$$

As pointed out by Nosrati-Ghods et al. 2020 [39], the impact of substrate limitation, substrate inhibition and product inihbition should be considered jointly. Among the 41 models presented in the review, only one model fulfilled this criteria and described the organism in question [43], however it only investigated kinetics of glucose and fructose co-fermentation. As such, to my knowledge no model has yet been proposed describing both substrate and product inhibition of glucose and xylose co-fermentation in *S. cerevisiae*.

2.5 CoRyFee

CoRyFee (Cost reduction in Yeast Fermentation for Commercial Production of Cellulosic Ethanol) is a recently developed continuous fermentation scheme developed by Sekab E-Technology AB (Sweden) and Terranol A/S (Denmark). It was designed for the purpose of maximizing ethanol productivity by monitoring sugar consumption and ethanol production in real-time [44]. The feed rate into a primary tank is continuously adjusted to maximize the rate of sugar consumption and ethanol production [18]. When the primary tank working volume is full, an outflow into the first holding tank is opened and set equal to the inflow in the primary tank (Figure 5). In media entering the holding tanks, most of the glucose has already been depleted and what remains are high concentrations of xylose, ethanol and biomass. The purpose of these holding tanks is maximizing the final yield of ethanol by allowing for complete fermentation of xylose. When the first holding tank is full the outflow from the primary tank is redirected to the second holding tank while the first holding tank is emptied and vice versa [18].

The refractive index (RI) of water (1.333 [45]) increases linearly with increasing concentration of sucrose [46] and this correlation is commonly used as a method of monitoring sugar content [47]. Applications of this method in other industries include determination of sugar content in horticultural products [48], estimates of serum immunoglobin levels in newborn calves [49] and characterization of honey from different bee-hive types [50]. In CoRyFee, this method is utilized by adjusting the feed rate so that the instantaneous RI derivative is minimized in the primary tank, maximizing ethanol production rate, while yield is maximized by allowing for ethanol production during a longer time in the holding tanks. The slow response of RI, unlike other indicators of fermentation progress such as carbon dioxide emission, yields a relatively stable signal suitable for feed rate control.

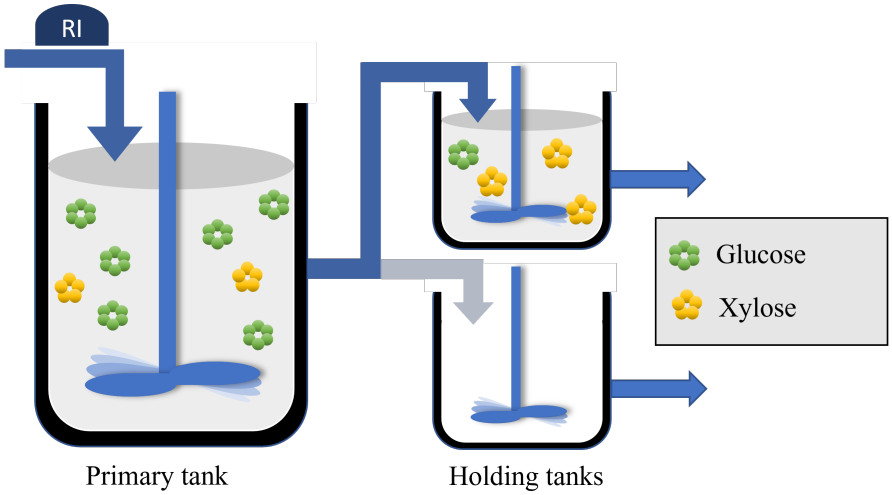

Figure 5: Schematic overview of the CoRyFee fermentation regime. The primary tank is run in fedbatch mode with RI feed rate control until the volume is full, then the outflow is opened to the first holding tank. The holding tank is also run in fedbatch mode, with the same feed rate as in the primary tank, until the volume is full.

3 Materials and methods

3.1 Inoculation and cultivation

Stock solutions of 200 gL^{-1} D-glucose (VWR Chemicals, Ohio, USA) and 200 gL^{-1} D-xylose (ITW reagents, Germany) were prepared by dissolving each component in demineralized water. 5x nutrient media with 33.5 gL^{-1} yeast nitrogen base (Beckton, Dickinson and Company, France), yielding a final concentration of 6.7 gL^{-1} according to manufacturer's recommendations, was also prepared with 50 mM succinic acid (VWR Chemicals, Belgium) as pH buffer and pH was adjusted to 5.5 through addition of 50 $\%$ potassium hydroxide (Merck, Germany). The composition of the final media used is summarized in Supplementary materials. All solutions were sterilized through autoclavation at 121 °C for 20 minutes. Dry cells of a proprietary xylose-fermenting strain of *S. cerevisiae* were hydrated in sterile tap water for 20 minutes prior to inoculation. After hydration, cells were immediately inoculated in 100 mL cultivation flasks with 25 mL liquid volume. Two replicates of each cultivation were used, one for measuring carbon dioxide loss and one for sampling. Cultivation flasks were sealed with a rubber lid and punctured with a sterile needle for carbon dioxide outflow. Cultures were incubated at 30 °C and 140 rpm shaking (LT-X incubator shaker, Kuhner AG, Switzerland) for approximately 30 minutes prior to the first sampling, carbon dioxide loss measurement and addition of absolute ethanol (VWR Chemicals, France). At the end of each incubation, cells were inspected under microscopy to ensure that no bacterial contamination had occurred.

3.2 Metabolite analysis

Fermentations were monitored real-time using weight loss as an indicator of carbon dioxide release, measured at a precision of 1 mg (Sauter RE 1614 Precision balance, Kern, Germany). Systematic errors due to evaporative weight loss were estimated, see Supplementary material.

600 µL samples were regularly withdrawn using a syringe, filtered through 0.45 nm HPLC filters (Econofiltr PTFE 13 mm 0.45 µm, Agilent Technologies, California, USA) and stored immediately at -80 °C. Sample analysis was performed using two different modes of High Pressure Liquid Chromatography (HPLC) (Dionex UltiMate 3000 Column Compartment, ThermoFisher Scientific, USA. First column: Shodex SH1011, mobile phase: 5 mM sulphuric acid. Second column: SP0810, mobile phase: milliQ water. Injection volume: 2 µL) with 1-isopropanol as internal standard. Concentrations of metabolites were determined by correlating chromatogram peak areas with known concentrations in a standard solution that was run as first and last sample in each analysis. Reference samples of xylitol (10 gL^{-1}) and succinic acid (20 gL^{-1}) were prepared and their respective elution retention times in the SP0810 column were determined as these were not included in the standard solution. Biomass formation was investigated using three different methods. First, cell pellet weight was determined by centrifuging 1 mL culture in an Eppendorf tube at 13 000 rpm for two minutes, discarding the supernatant through pipetting, weighing the tube and subtracting the weight of the empty tube. Second, absorbance was measured at 600 nm for samples diluted to fit the linear range of the spectrometer. Third, nitrogen assimilation was estimated based on change in pH. pH was determined in three replicates before incubation and after glucose had been depleted (approximately 5 hours after inoculation) as an estimate of ammonium sulphate consumption, the nitrogen of which was assumed to only be used for protein production.

3.3 Determination of cell viability

Investigation of cell viability was performed by MoRe Research (Örnsköldsvik, Sweden). Cell viability was estimated both among the hydrated dry cells used at inoculation, as well as among overnight cultivated cells exposed to 14, 28 or 60 gL^{-1} ethanol. Cultures were prepared with 2 gL^{-1} dry cells, 50 gL^{-1} glucose and nutrient media (1x), then incubated overnight at 30°C and 140 rpm. After incubation, the cell dry weight was estimated in three replicates by centrifuging 1 mL culture for 2 minutes at 13 500 rpm, discarding the supernatant and weighing the cell pellet. The original culture was aliquoted into 1 mL samples and centrifuged with the same settings. The supernatant was discarded and the cells resuspended in 1 mL sterile tap water. Four additional samples were prepared with 25 gL^{-1} freshly hydrated cells as reference. Samples were kept on ice throughout remaining preocedure. For microscopy, three replicates were prepared of each sample. 0, 13, 28 or 60 gL^{-1} ethanol was added to the overnight incubated samples and 0 or 28 gL^{-1} ethanol was added to the freshly hydrated cells 10 minutes before analysis. Chlorine was added to a regular Baker's yeast sample as control. For each replicate, a droplet of cell suspension was transferred to a glass slide and stained with 0.1 $\%$ methylene blue. Excess liquid was removed and the remaining was covered with a cover glass. Each slide was investigated using a light microscope in regular and phase contrast mode.

3.4 Experimental overview

Table 3 summarizes which cultivations were run throughout this project. Three levels of glucose, xylose and ethanol were used in different combinations. When xylose was used as sole carbon source, two datasets (hour 1 to 10 and hour 15 to 25) were merged because an increased amount of fermentation time was required to reach xylose depletion. In one experiment, the ethanol was

added after five hours instead of from the begnning.

Cells (gL^{-1})	Glucose (gL^{-1})	Xylose (gL^{-1})	Ethanol (gL^{-1})	Replicates (n)	Time (h)	Notes
25	25	25	0, 20	2	10 hours	-
25	25	0	0, 20	1	10 hours	-
25	0	25	0, 20	2	25 hours	Merged data
25	25	50	0, 20, 40	1	10 hours	-
25	25	50	0, 20, 40	1	10 hours	Delayed etOH addition
25	10	50	0	1	10 hours	-

Table 3: Overview of experimental design. **Merged data**: data from two separate experiments were merged into one plot for practical reasons (hour 0 to 10 and hour 15 to 25 are two different cultures). **Delayed etOH addition**: ethanol was added when glucose was estimated to be depleted (after 5 hours of incubation)

3.5 Model formulation

A simple kinetic model of glucose and xylose fermentation is illustrated in Figure 6, where q1, q2, q3 and q4 are rate expressions for glucose uptake, xylose uptake, ethanol formation and growth, respectively. All variables included in the model, except biomass, are measurable using HPLC.

Figure 6: Fermentation model for *S. cerevisiae* glucose and xylose co-fermentation.

No previously proposed kinetic model was found that simultaneously describe both glucose inhibition on xylose uptake and ethanol inhibition on metabolic activity. Additionally, the expected inhibitory effect of ethanol on xylose fermentation has been poorly investigated. Due to the lack of comprehensive and validated models, a combination of previously suggested kinetic models was used throughout this study. Importantly, the formulation of a kinetic model including all inhibitory relationships of interest requires further investigations than what is covered in this study, and the model should therefore not be considered generally valid. Equation (1) was combined with equations (2) and (3) to form a model including both substrate and product inhibition, resulting in equation (5) and (6). A phase shift occurring when glucose drops below a limit value *alpha* was included that results in a changed ethanol yield on sugar (equation (8)), according to a previously presented model. Unlike previously presented models, the biomass yield was set to be the difference in theoretical yield and actual yield of ethanol (equation (9)). The biomass yield is in the unit grams biomass per grams glucose based on the average molar mass of yeast $M_{biomass}$ = 26.09 g/C-mol [51]. The ethanol and biomass yields were assumed to be equal for glucose and xylose.

$$\frac{dGlu}{dt} = -vmax1 * X * \frac{glu}{K1 + glu} * \left(1 - \frac{E}{E_{max}}\right)^{a} * \left(1 - e^{\frac{-t}{tau}}\right) \tag{5}$$

$$\frac{dXyl}{dt} = vmax2 * X * \frac{xyl}{K2 * (1 + \frac{glu}{K_{glu}})} * \left(1 - \frac{E}{E_{max}}\right)^{a} * \left(1 - e^{\frac{-t}{tau}}\right) \tag{6}$$

$$\frac{dP}{dt} = -\left(\frac{dGlu}{dt} + \frac{dXyl}{dt}\right) * Y_{ps} \tag{7}$$

$$Yes = \begin{cases} Yes1 & \text{if } glu > alpha \\ Yes2, & \text{if } glu \leq alpha \end{cases} \tag{8}$$

$$Y_{xs} = (Y_{es}^{max} - Y_{es})/M_{etOH} * 2 * M_{biomass} \tag{9}$$

Simulations of batch mode fermentations were performed in Matlab v. 9.10.0 (R2021a) (Mathworks, Natick, MA, USA) by solving the initial value problem using the *ode15s* function. Resulting concentrations of glucose, xylose and ethanol were plotted against time.

3.6 Model parameter estimation

HPLC data of glucose, xylose and ethanol concentrations (gL^{-1}) were imported from Microsoft Excel (2019) into MatLab. Time data were converted from minutes to hours and *n.a.* values were set to zero for all data sets. Initial concentrations for the model were defined as the first measurements in the experimental data and initial parameter values were chosen arbitrarily. The MatLab function *fminsearch* was used to minimize the sum of squares of the difference between experimental and simulated data by varying parameter values with a maximum number of evaluations set to 5 000. Resulting parameter values are presented in Supplementary material. Coefficients of determination (r^2) for the modelled and experimental data were calculated using the *corrcoef* function.

3.7 CoRyFee simulation

The simulation code was modified to represent the CoRyFee technology applied in a continuous fermentation regime. A *for loop* was designed where each iteration represents a measurement by the RI monitor (see code below). The initial value problem was solved between each measurement, and the concentrations of glucose, xylose, ethanol and biomass after each iteration were saved in a sampling vector. The RI value at a specific ethanol concentration was extracted from a randomly generated exponential curve correlating ethanol concentration and RI. The derivative of RI (*dRI*) was calculated as the difference between the latest and the antecedent RI value. If the current *dRI* was smaller than the previous *dRI*, then the change in flowrate had a positive impact and an equally large change was made in the same direction. If on the other hand the current *dRI* was larger, the flowrate was reset to its previous value and the direction of change inverted. In the simulation,

a primary tank (10 L) was first run in fed-batch mode with an initial biomass concentration of 5 gL^{-1}. The feed rate was controlled based on RI to maximize ethanol production. When the tank volume was full, an outflow was opened and set as inflow into one of the holding tanks (5L). The initial volume of each tank was set to 10 $\%$ of its full volume.

```
for k = 2:(200*20)    % Sampling every third minute for 200 hours
    RI(k) = r(E(k))   % Withdraw RI value at current ethanol level
    dRI(k) = RI(k) - RI(k-1)    % Calculate dRI(k)
    if dRI(k) <= dRI(k-1) % If the new dRI is smaller than or
                            equal to the previous one
        flowrate(k+1) = flowrate(k) + C  % Change the flowrate
                                           in the same direction
    else            % Otherwise
        flowrate(k+1) = flowrate(k)   % Reset to previous flowrate
        C = C*(-1)      % Change the flowrate in the opposite
                          direction next time
end
```

4 Results

4.1 Experimental results

A commercially available strain of xylose fermenting yeast was inoculated with glucose, xylose or a combination of both and was allowed to ferment for approximately 10 hours. Below, the fermentation rate based on CO_2 loss and consumption profiles of sugar are presented when glucose and xylose are co-fermented and when xylose is used as sole carbon source. Maximum specific sugar consumption rates, ethanol yields and glycerol yields using the different carbon sources are summarized. Finally, an estimation of cell viability and biomass formation during glucose consumption is presented.

4.1.1 Glucose and xylose co-fermentation

Two replicates were inoculated in defined media with 25 gL^{-1} cells and an equal concentration of glucose and xylose (25 gL^{-1}). The fermentative rates were monitored based on weight loss, which was assumed to correlate with carbon dioxide formation and thus to fermentative rate. Figure 7 shows the average ethanol concentration (**A**) and weight loss (**B**) of cultures with 0 or 20 gL^{-1} added ethanol. During the first six hours, the culture with added ethanol ferments slower than the culture without added ethanol. After six hours, deviations were too large to observe a difference. Weight loss data rendered smoother curves than HPLC-based ethanol data.

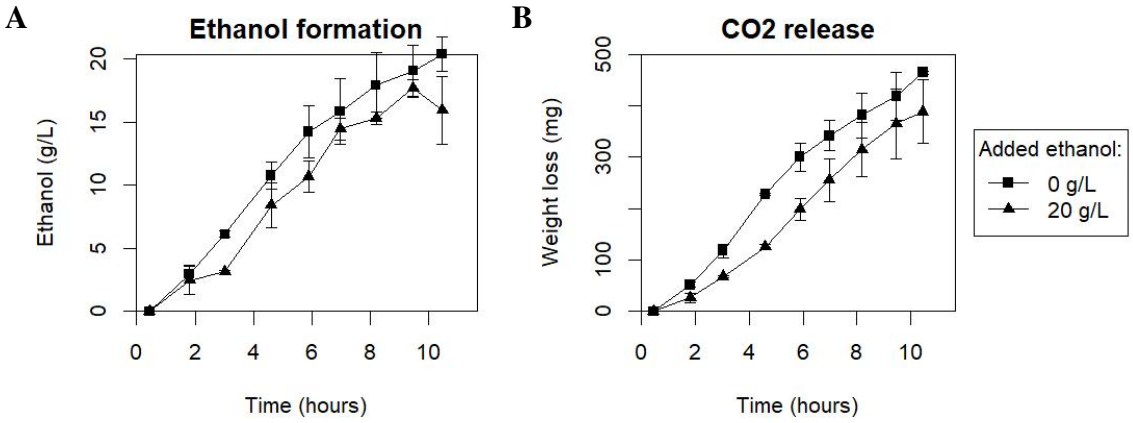

Figure 7: Average eEthanol formation and carbon dioxide release with 0 or 20 g/L initially added ethanol estimated based on two replicates of glucose and xylose co-fermenting cultures.

Sugar consumption was monitored during fermentation through regular sampling and HPLC analysis. Initially, glucose was consumed almost exclusively and at a slower rate in the cultures with added ethanol (Figure 8**A**). Although large deviations between replicates were observed in this data as well, maximum rates of xylose consumption appeared similar regardless of ethanol addition, but were delayed in the cultures with added ethanol (Figure 8**B**).

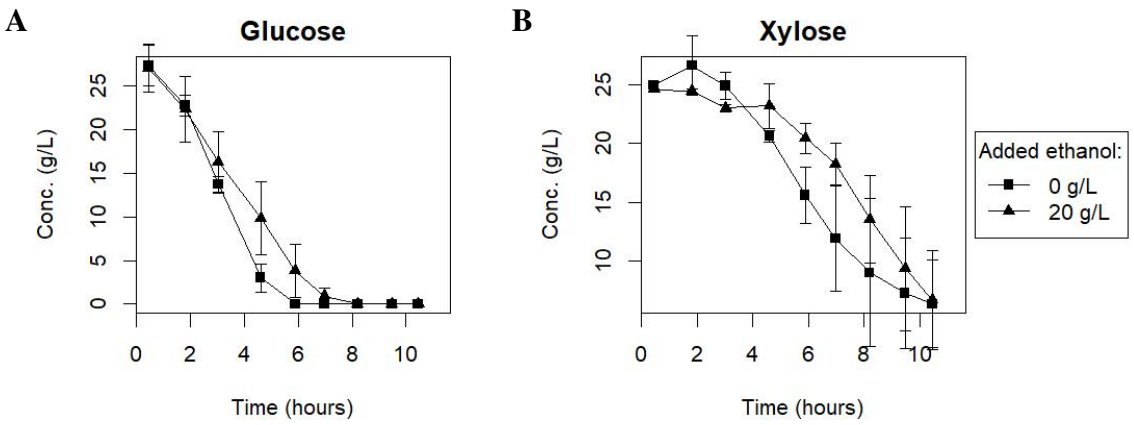

Figure 8: Average concentration of glucose (A) and xylose (B) over time in two biological replicates of co-fermenting cultures with and without addition of 20 g/L ethanol.

4.1.2 Xylose as sole carbon source

Cultures were incubated in two biological replicates during 24 hours with xylose as the only available substrate (Figure 9). Initially, no difference between cultures with and without ethanol was observed. After a lag phase of approximately 15 hours an exponential phase began, although the time of onset differed both between the cultures with and without ethanol, as well as between the two replicates.

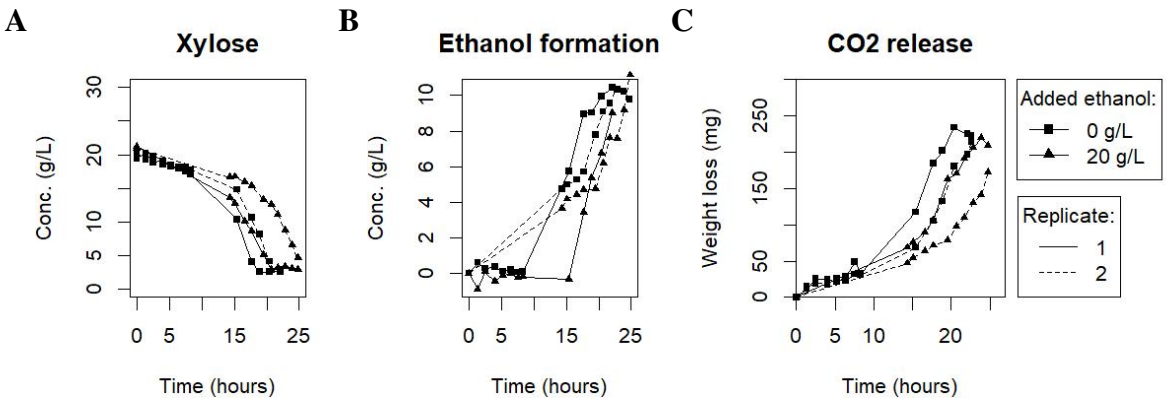

Figure 9: Xylose consumption (**A**), ethanol formation (**B**) carbon dioxide release (**C**) in two biological replicates when only xylose is provided as carbon source.

4.1.3 Carbon consumption rates and ethanol yields

Maximum specific consumption rates ($g\ g_{DCW}^{-1}\ L^{-1}$) and balanced ethanol yields (the amount of formed product divided by the difference between initially added substrate and remaining substrate at the end) of glucose and xylose fermented individually and together are summarized in Table 4. The maximum rate of glucose consumption, when given as sole carbon source, was reduced by on average 16.5 $\%$ when ethanol was added. No difference in consumption rate was observed when ethanol was added to a culture given xylose as sole carbon source. In co-fermenting cultures, a decrease in glucose consumption rate was observed (22 $\%$) while the xylose consumption rate

increased by on average 33 %. With xylose as sole carbon source, yields of ethanol were above theoretical maximum (0.51). In co-fermenting cultures, lower yields of ethanol were observed compared to when xylose was consumed as sole carbon source. The ethanol yield was reduced when ethanol was added to the co-fermenting culture, but remained almost the same when ethanol was added to a culture with glucose as sole carbon source.

Glucose	**Xylose**	**Ethanol**	**Max. glucose rate** ($\mathbf{g\ g^{-1}_{DCW}L^{-1}h^{-1}}$)	**Max. xylose rate** ($\mathbf{g\ g^{-1}_{DCW}L^{-1}h^{-1}}$)	**Yield ethanol** ($\mathbf{g\ g^{-1}}$)
+	-	-	0.25		0.41
+	-	+	0.21		0.42
-	+	-		0.09 (0.02)	0.53 (0.01)
-	+	+		0.10 (0.01)	0.57 (0.12)
+	+	-	0.22 (0.01)	0.08 (0.01)	0.45 (0.03)
+	+	+	0.17 (0.01)	0.11 (0.01)	0.35 (0.01)

Table 4: Maximum specific sugar consumption rates and ethanol yields of glucose and xylose fermented individually or simultaneously with or without ethanol added initially (mean (standard error)). "-" indicates absence and "+" indicates presence of compound (25 gL^{-1} for glucose and xylose, 20 gL^{-1} for ethanol). All samples have equal amounts of nutrients and 25 gL^{-1} biomass.

4.1.4 Addition of ethanol after glucose depletion

The concentration of xylose was doubled to 50 gL^{-1} and cultures were spiked with ethanol initially and after glucose depletion (dashed line) (Figure 10). Specific fermentative rates during xylose consumption were similar with and without addition of 20 g/L ethanol (0.944 and 0.945 $gg^{-1}L^{-1}$, respectively) when added initially (Figure 10A). When ethanol was added after glucose depletion, however, a decrease in specific fermentative rate was observed in the xylose-consuming phase (0.713 $gg^{-1}L^{-1}$) (Figure 10B). The fermentative rate was reduced even more when 40 gL^{-1} ethanol was added.

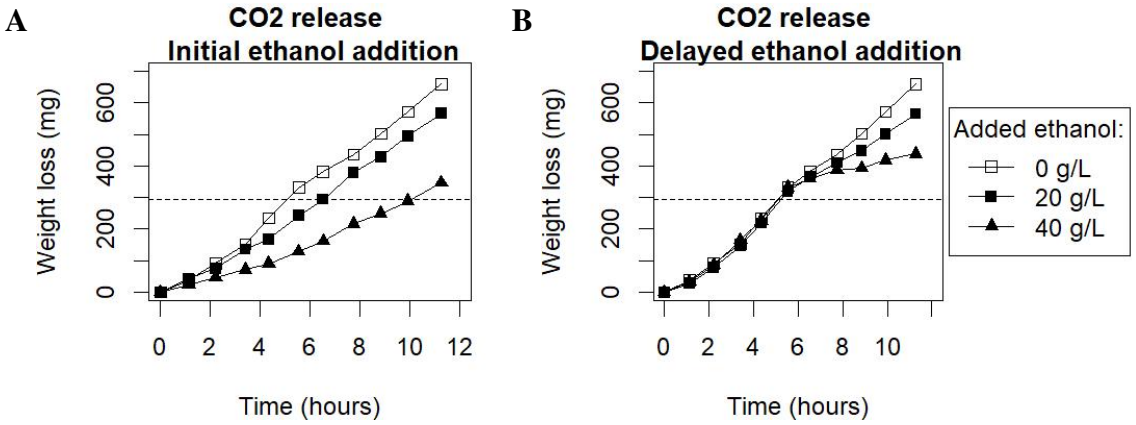

Figure 10: Carbon dioxide release estimated based on average weight loss for cultures with 25 gL^{-1} glucose, 50 gL^{-1} xylose and 0, 20 or 40 gL^{-1} ethanol added initially (**A**) or after glucose depletion (**B**). Dashed lines mark glucose depletion.

4.1.5 Biomass formation

Biomass formation was investigated using several methods, but conclusive results were obtained only from the method of measuring assimilated nitrogen. As shown in Table 5, a higher final pH was observed when 20 gL^{-1} ethanol was added initially, indicating a reduced nitrogen assimilation and thus suppression of growth.

Initial ethanol	**0 min**	**300 min**
0 gL^{-1}	5.60	4.01
20 gL^{-1}	5.61	4.24

Table 5: pH of fermentations before incubation and after 5 hours, when glucose is assumed to be depleted.

pH values were used to calculate the amount of protons released and thus the amount of nitrogen assimilated into biomass (see Supplementary material). Calculations were based on the assumptions that each nitrogen atom is bound to four protons, one proton is bound by the sulphate ion upon release and that 8 $\%$ of total yeast biomass consists of nitrogen. The absolute amount of formed biomass based on nitrogen assimilation was found negligibly low, 126.7 and 73 mg for 0 and 20 gL^{-1} added ethanol, respectively. This difference could be caused by a varying amount of viable cells between the cultures.

4.1.6 Cell viability after ethanol addition

Dry cells hydrated for 30 minutes (Figure 11) and overnight cultivated cells (Figure 12) were stained and studied in microscope to investigate whether ethanol had an impact on cell viability. Blue cells are metabolically inactive and assumed to be non-viable. Among the hydrated cells, an estimated 70 $\%$ of the cells were found viable but significantly smaller in size compared to cultivated cells. An estimated 5-10 $\%$ cells were dead among the overnight cultivated cells. Living cells were large and most of them were in the state of mitosis, indicating a healthy population. No difference in quotient of dead cells was observed when 14 or 28 gL^{-1} ethanol was added, neither after 10 nor 30 minutes. When 60 gL^{-1} ethanol was added, the quotient of dead cells increased to approximately 30 $\%$ (data not shown). Chlorine was added to regular baker's yeast as control, displaying an essentially 100 $\%$ cell death within the first 2 minutes of exposure (data not shown).

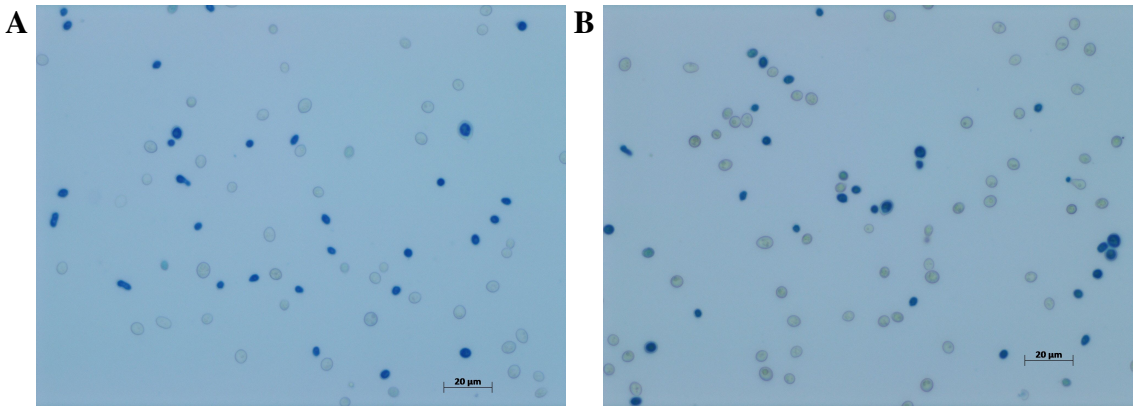

Figure 11: Recently hydrated cells stained with methylene blue 10 minutes prior to the time of the picture. **A**: No added ethanol, **B**: 28 gL^{-1} added ethanol.

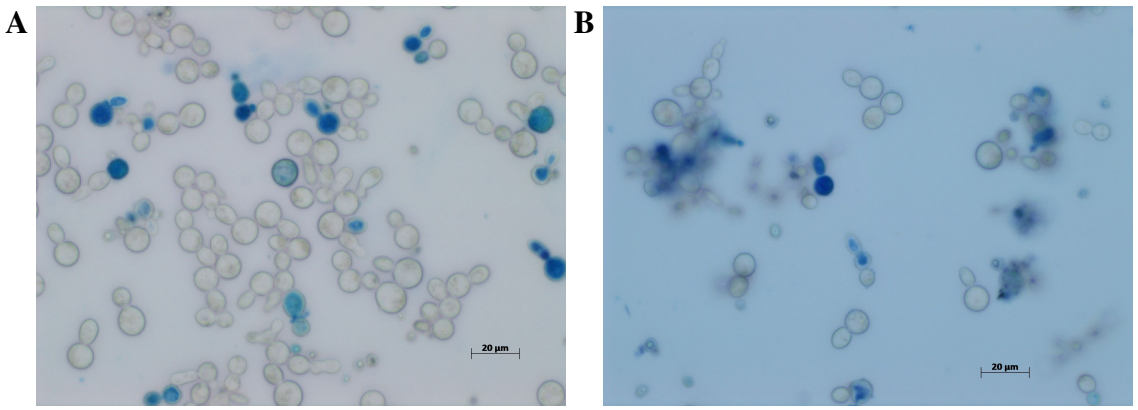

Figure 12: Overnight cultivated cells stained with methylene blue 10 minutes prior to the time of the picture. **A**: No added ethanol, **B**: 28 gL^{-1} added ethanol.

4.2 Computational results

A simple model including glucose, xylose, ethanol and biomass as variables was suggested, although the kinetic expressions need further verification. Kinetic parameters were optimized to fit experimental batch data for fermentations with two different xylose levels. First, the model proposed by Taumala et al. 2016 was optimized to data from fermentations without added ethanol. Second, the model suggested in section 3.5 was optimized to data from fermentations that also included four different ethanol levels (0, 10, 20 and 40 gL^{-1}). Optimized parameter values for both models are presented in Supplementary materials. Finally, the suggested model was implemented in a CoRyFee simulation with an RI based feed-rate control algorithm.

4.2.1 Model fit without ethanol addition

Two independent fermentation datasets without ethanol addition were fitted to the model proposed by Taumala et al. 2016 (Figure 13), with 25 gL^{-1} inoculated biomass and sugar concentrations according to the figure. Average coefficients of determination (R^2) describing how well the simulated data fit the experimental data were 0.997, 0.982 and 0.995 for glucose, xylose and ethanol,

respectively. This model assumed different ethanol yields depending on whether the glucose concentration was larger or smaller than a limit value *alpha*, and these were predicted to be 0.379 g/g and 0.467 g/g before and after glucose exhaustion, respectively (see Supplementary materials). These correspond to 74 % and 92 % of theoretical maximum.

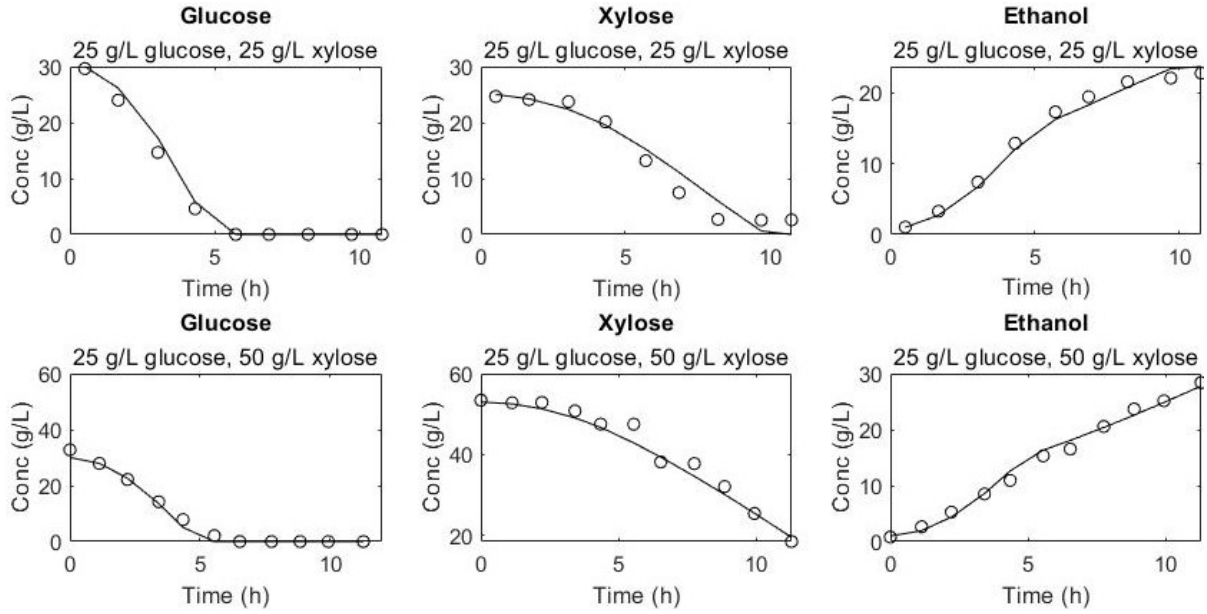

Figure 13: Kinetic model fitted to experimental data with 25 gL^{-1} glucose, 25 or 50 gL^{-1} xylose and 25 gL^{-1} biomass.

A dataset with reduced initial glucose concentration (10 gL^{-1}) and increased inoculated biomass concentration (50 gL^{-1}) was used for validation (Figure 14). The model performed well in predicting behaviour during glucose fermentation, but a pause in fermentation during xylose consumption (hour 5 to hour 7) occurred in the experimental data that was not predicted by the model. R^2 values were determined to 0.953, 0.959 and 0.951.

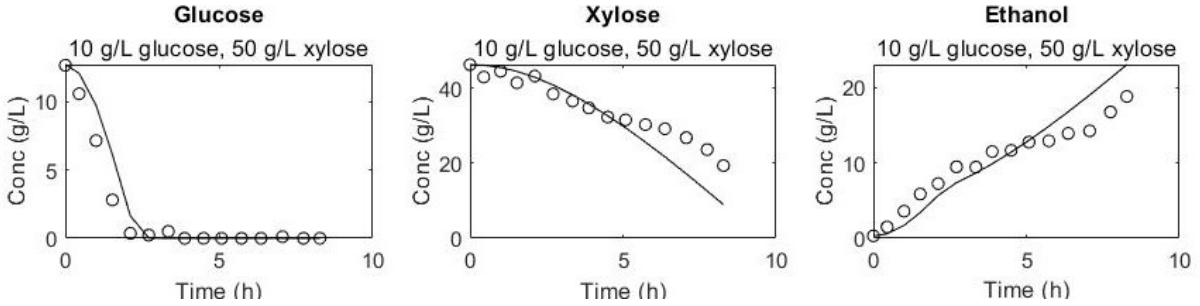

Figure 14: Comparison of model-predicted behaviour to dataset at which the model has not been trained on.

4.2.2 Model with ethanol-induced inhibition

The ethanol inhibition factor suggested by Levenspiel et al. 1980 was added to the glucose and xylose kinetic expressions and experimental data with 20 gL^{-1} and 40 gL^{-1} added ethanol were

included when fitting the model. This resulted in R^2 values of 0.993, 0.931 and 0.976 for glucose, xylose and ethanol, respectively. The model performs well in simulating glucose fermentation but poorly in predicting xylose fermentation (Figure 15). The ethanol yields were similar as in the model without ethanol inhibition (0.372 and 0.436 g/g)). 86 gL^{-1} was predicted to be the ethanol concentration limit beyond which no metabolic activity occurs (E_{max}).

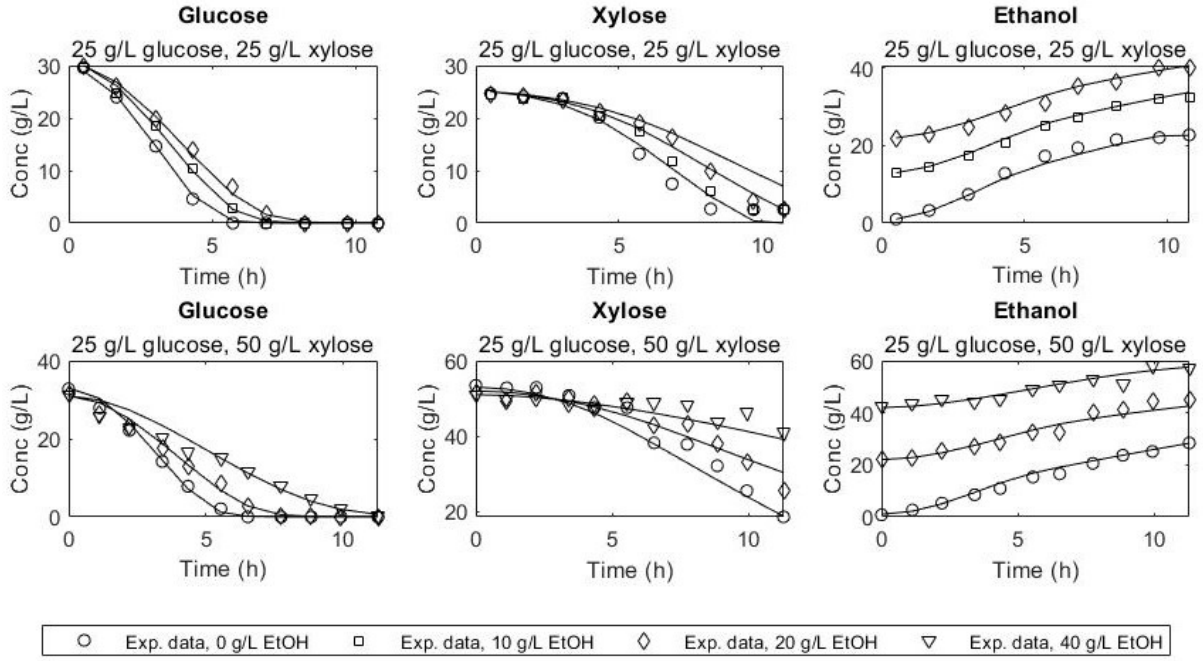

Figure 15: Kinetic model fitted to experimental data with different levels of ethanol added initially.

4.2.3 Modelling CoRyFee

The model was implemented in a continuous simulation code representing the CoRyFee technology (Figure 16). Fluctuations of sugar concentrations in the feed were simulated by randomly extracting values from a normal distribution with $\mu = 25$ and varying σ values. A steady value of RI was maintained by the algorithm when $\sigma \leq 5$. Fermentation in the primary tank was first run in fed-batch mode, during which ethanol and biomass concentrations increased exponentially. When the reactor was filled (10 L), an outflow equal to the inflow was opened into a holding tank and the primary tank entered a continuous mode. Once the primary tank had entered continuous mode, glucose and xylose levels were maintained close to depletion. Ethanol and biomass eventually set at concentrations of approximately 10 gL^{-1} and 4 gL^{-1}, respectively, and a minimum value of RI was found to be $\sim$0.24. Average feed rate during the continuous fermentation in the primary tank was determined to 0.1128 Lh^{-1}.

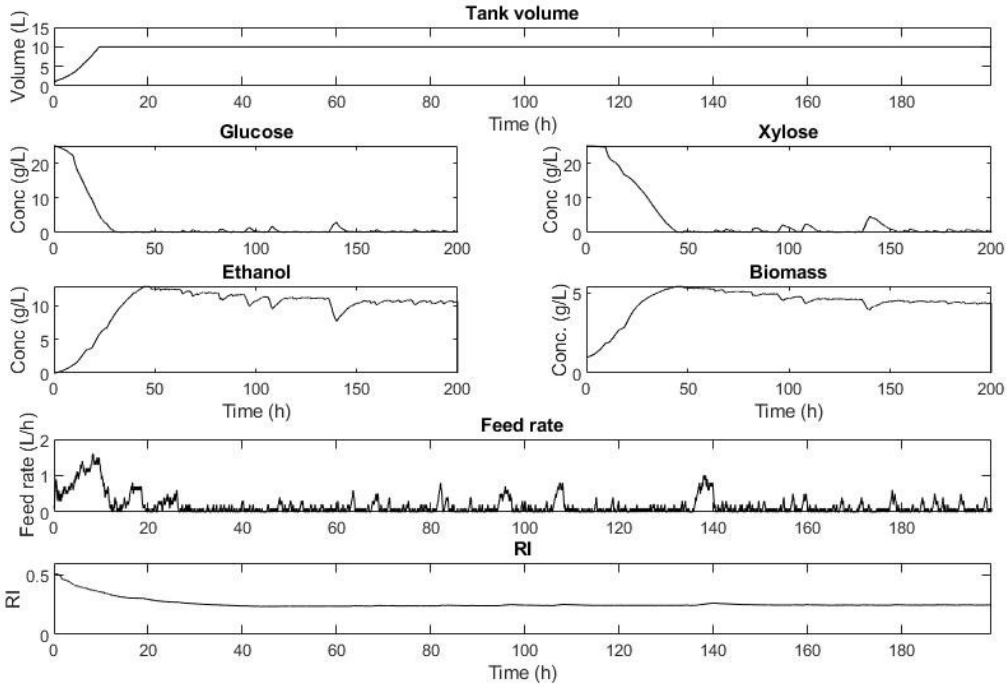

Figure 16: Simulation of CoRyFee with fluctuating glucose and xylose feed concentrations with $\mu = 25$ and $\sigma = 5$.

The model was found highly sensitive to changes in parameter values. In particular, RI sampling and flowrate adjustment frequencies had a large influence on the behaviour of the algorithm. In the simulation presented, sampling was set to occur every 20 minutes. If sampling frequency was reduced, the feed rate would gradually decrease and set at a very low rate. Increased sampling frequency resulted in large fluctuations in the flow rate and irregular patterns of concentrations.

5 Discussion

The task requested by Sekab was to investigate how external addition of ethanol impacts fermentative rate during glucose and xylose co-fermentation. Their interest in ethanol originate from a recently observed technical effect that fermentation of lignocellulosic hydrolysates speeds up towards the end if ethanol has been added initially. Below follows a discussion addressing different theories about how xylose metabolism is affected by glucose and ethanol during co-fermentation, as well as an evaluation of performance of the CoRyFee simulation and suggested future improvements.

5.1 Investigation of cellular mechanisms

Fermentation progress was monitored on-line through estimation of carbon dioxide release. The gradual weight loss of cultivations was assumed proportional to the fermentative rate as a result of carbon dioxide being formed during ethanol formation and released through the sampling syringe. This method has previously been demonstrated to agree well with HPLC data [52]. To further confirm the validity of this method, an estimation of the evaporative impact was performed (see Supplementary material). Curves rendered from weight loss data were generally smoother than HPLC-based ethanol data, however large deviations between replicates were observed with both methods (Figure 7). This inconsistency made it difficult to draw conclusions from the available data, and more experiments are needed in order to demonstrate that ethanol added initially has a positive effect on xylose fermentation rate. Nevertheless, within each individual experiment the maximum fermentative rate during xylose fermentation was similar with and without ethanol, while the maximum fermentative rate of glucose was consistently lower in the culture with 20 g/L ethanol compared to the one without ethanol (Table 4).

High cell density cultivations allow for a shorter fermentation time and higher volumetric productivity [53]. Therefore, a higher initial biomass concentration (25 gL^{-1}) compared to similar reports ([31] [29] [26]) was used in this study. However, this caused complications in measuring biomass concentration. Cell density measurements were made by weighing cell pellet obtained through centrifugation of 1 mL culture and removal of the supernatant by pipetting, but deviations between repeated measurements were too large to identify differences between biological samples. Measurements of absorbance at OD_{600} rendered the same issue, likely because the cells sedimented too quickly in the original culture and the drawn sample was therefore not representative. The final method used, correlating pH decrease to growth based on protons released from ammonia during nitrogen assimilation, rendered statistically significant results but indicated that growth occurred at a negligible rate (section 4.1.5). If that is the case, it could explain why no difference could be observed in the dry cell pellet weight measurements. Consequently, growth was not monitored in remaining experiments. An investigation of cell viability at inoculation was however performed by staining recently hydrated cells with methylene-blue. It became evident that, among the dry cells inoculated, only 70 $\%$ were viable (Figure 11). Consequently, initial biomass concentrations were 17-18 gL^{-1} rather than 25 gL^{-1} and maximum specific sugar consumption rates were consistently underestimated. However, as consumption rates were only evaluated relative to experiments with the same systematic error, this did not have an impact on any conclusions drawn from this data.

5.1.1 Increased xylose fermentation rate in co-cultures with added ethanol

The increased fermentative rate during xylose consumption that Sekab observed when adding ethanol could not be proven in defined media with the currently used method due to large deviations between replicates. When ethanol was added, cultures consumed glucose at a lower specific rate (on average 0.171 compared to 0.219 $g\ g^{-1}L^{-1}$) and started fermenting xylose later (Figure 8). However, the maximum xylose consumption rate was found higher on average in the cultures with added ethanol (on average 0.109 compared to 0.082 $g\ g^{-1}L^{-1}$). At a higher xylose concentration (50 gL^{-1}), xylose consumption rate was similar with and without ethanol addition (Figure 10**A**).

5.1.2 Impact of prolonged glucose availability on xylose transportation kinetics

Xylose uptake is known to be highly dependent on glucose abundance, both because glucose regulates the expression of *HXT* genes and because glucose and xylose compete for interaction with *hxt* proteins. Generally, *hxt* proteins have a higher affinity for glucose than xylose, resulting in a competitive imbalance and negligible uptake of xylose at high glucose concentrations. Expression of different *HXT* genes with varying glucose and xylose affinities is also highly dependent on glucose levels: high-affinity *hxt* proteins have been demonstrated repressed at high glucose levels as well as when glucose is absent. Xylose uptake is therefore expected to be optimal at low but non-zero levels of glucose. A hypothesis explaining the increased rate of xylose fermentation in ethanol-spiked cultures could be that glucose fermentation is inhibited, prolonging glucose availability at low concentrations. Assuming some delay in *HXT* down-regulation due to glucose depletion, this hypothesis could explain the behaviour observed in Figure 8. However, at 50 gL^{-1} xylose the fermentation rate remained constant long after glucose was depleted. Additionally, a similar maximum xylose consumption rate was eventually observed when xylose was given as sole carbon source. Thus, repression of high-affinity *HXT* genes due to absence of glucose does not seem to cause a reduction in maximum xylose consumption rate, and prolonged glucose availability is therefore an implausible explanation to the increased fermentative rate observed when ethanol is added.

5.1.3 Delay of xylose fermentation

A $\sim$15 hour delay of xylose consumption onset was observed when xylose was given as sole carbon source (Figure 9**A**). A similar behaviour was observed by Saloheimo et al. 2007 [31], although lasting for several days. This difference may be due to the highly different initial biomass concentrations used, 25 gL^{-1} in the present study compared to an OD of 0.2 or 1 in the study by Saloheimo et al. 2007. Assuming a correlation found in literature between optical density and dry weight (1 OD_{600} = 0.62 gCDW/L [54]), the initial biomass concentration used presently was 40x or 200x higher compared to the initial biomass concentration used by Saloheimo et al. 2007. Furthermore, when Golcalves et al. 2014 [29] studied xylose transportation and *HXT* regulation no delayed xylose consumption was observed. This was probably because their experiments were based on a time frame of 70 hours, the time at which cultures are still expected to be in an elongated lag phase with the initial OD_{600} used (1.1 $\pm$ 0.4). An explanation to this delay could be lack of xylose catabolite sensing. When glucose is present, transportation mechanisms and glycolytic pathways are activated through the sensing by rgt2 and snf3 [55] and subsequently

utilized for xylose metabolism. In absence of glucose, such activation likely does not occur and xylose metabolism proceeds at a slow rate. After a certain amount of time (15 hours), however, the cells start consuming xylose at the same rate as when glucose had been present, possibly due to some slow adaptation of snf3 and rgt2.

5.1.4 Carbon allocation between ethanol and growth

Another hypothesis was that addition of ethanol influences carbon allocation between ethanol and growth. Table 4 shows that the ethanol yield was $\sim$80 $\%$ of theoretical maximum when glucose was given as sole carbon source, but roughly equal to theoretical maximum (slightly overestimated) for xylose fermentation. During glucose and xylose co-fermentation with added ethanol, an ethanol yield of only 69 $\%$ of theoretical maximum was obtained, indicating that carbon must have been partially allocated elsewhere. One such carbon-consuming process is growth, requiring carbon both for biomass formation and, if under anaerobic conditions, glycerol formation. However, estimations of biomass formation from nitrogen assimilation indicated that growth occurred at a negligible rate during glucose consumption. The hypothesis that growth is the explanation to the ethanol effect was therefore deemed implausible. Another possible cause of reduced ethanol yields when external ethanol is added is the formation of other metabolic byproducts. HPLC chromatograms were therefore scavenged for organic acids, xylitol or other unknown components. Some acetic acid was identified in most samples, but at insufficient levels to have a significant impact on overall carbon allocation. No other components beyond those added to the cultivation media were identified. A third explanation is that more ethanol had evaporated in the experiments with lower ethanol yields, however the investigation of evaporative impact presented in Supplementary materials does not support this explanation.

5.1.5 Nutrient starvation

Adding ethanol may result in reduced utilization of nutrients during the glucose consuming phase due to inhibition, hence more nutrients would be left for the xylose consuming phase leading to increased growth rate. However, this theory was also ruled out as a very low amount of nitrogen was assimilated compared to the amount added («1 gL^{-1} compared to 6.7 gL^{-1}).

5.1.6 The temporary inhibition theory

Surprisingly, ethanol caused a reduced xylose fermentation rate when it was added after glucose depletion (Figure 10B). This could suggest that ethanol has a temporary negative effect on cells regardless of when it is added and what type of carbon source happens to be consumed at that time point. Ethanol is known to be toxic to cells and strains used in industrial fermentations have therefore been selected for high ethanol tolerance. When the ethanol level surrounding the cells gradually increase as a result of fermentation, there is time for the cells to adapt to the increased toxicity. However, a sudden increase in ethanol likely constitute a shock to the cells and the culture may require some time to recover and adapt. Cultures to which ethanol was added initially may consequently be better adapted for high ethanol concentrations compared to those without initial ethanol addition, which could explain their increased fermentative rate towards the end. At the ethanol levels investigated, however, a correlation between added ethanol and reduced cell viability

measured using methylene-blue could not be demonstrated. Further investigation is needed before this hypothesis can be confirmed or discarded.

5.1.7 Kinetic modelling reveal insufficient understanding of ethanol-induced xylose fermentation behaviour

Fermentations were performed *in silico* using differential equations describing how concentrations of glucose, xylose, ethanol and biomass change over time. The model proposed by Taumala et al. 2016 could well represent experimental data when glucose and xylose were co-fermented with 25 gL^{-1} inoculated biomass and without addition of external ethanol (Figure 13). Adding an ethanol inhibition factor adapted from the model proposed first by Levenspiel et al. 1980 rendered an accurate simulation of ethanol inhibition on glucose fermentation, but did not fit as good with the xylose data (Figure 15, R^2 = 0.931 for xylose compared to R^2 = 0.993 for glucose). Increasing the maximum number of iterations for solving the ODE did not significantly impact the results.

In the present study, biomass yields were set to be the difference between theoretical maximum and observed yield of ethanol. This deviation from previously suggested models was made in order to circumvent the lack of consistent biomass measurement data. However, biomass yield is likely highly dependent on biomass concentration and possibly other environmental factors. The model is therefore inapplicable on fermentations with, for example, lower inoculated biomass concentration. Furthermore, neither of the models was able to predict the rate of xylose fermentation in the validation dataset (Figure 14), which had a higher initial biomass concentration (50 gL^{-1}) and a lower glucose concentration (10 gL^{-1}). In this setting, a temporary decrease in xylose fermentation rate occurred after 5 hours. This behaviour has been reported previously [31], although in an *hxt null* strain engineered with only one *HXT* gene and over a longer timespan than what is presented here. Moreover, when xylose was given as sole carbon source an approximately 15 hours long delay of xylose fermentation occurred. Neither of these observations was predicted by the models. A way to account for the latter could be by introducing separate lag phase constants for glucose and xylose. However, widely different lengths of the xylose lag phase were observed in this report compared to Saloheimo et al. 2007 and Goncalves et al. 2014. The lag phase constant for xylose is therefore expected to be highly dependent on other factors such as glucose concentration and inoculated biomass concentration. Until a correlation is proposed between the time it takes for xylose consumption to enter an exponential phase and other fermentation conditions, it will not be possible to model this effect with the currently used method.

5.2 Simulating CoRyFee

An algorithm implementing RI-based feed rate control of a continuous CoRyFee fermentation regime was successfully designed using the model with ethanol-induced inhibition. The algorithm managed to maintain a steady process despite random variations in glucose and xylose concentrations in the feed ($\mu = 25, \sigma = 5$) (Figure 16), demonstrating that RI measurement is a robust method for feed rate control. However, the model also indicated that a second holding tank for xylose consumption would be unnecessary, as maximum ethanol production was obtained while both glucose and xylose were depleted. In real CoRyFee simulations, however, RI-based flow rate control results in a non-zero xylose concentration in the outflow of the primary tank, thus

the need for a holding tank. In order to simulate this, a drastic decrease in xylose consumption rate (either by increasing $K2$ or decreasing $v_{max,2}$) would be required. As such, it is likely that xylose consumption in real CoRyFee settings progresses slower than what is observed in the batch cultures performed in this study. This could be due to numerous factors. Firstly, hydrolysates provide a very complex environment for the cells with several available carbon sources, inhibitory compounds and possibly contaminating agents that must be taken into account. Secondly, a kinetic model optimized for batch cultures may not be directly transferable to continuous regimes. To adjust for this, parameter re-optimization could be performed on data from a continuous setup. Finally, the kinetic model used is relatively simple and several improvements are required for an accurate representation of relevant conditions. The currently used model assumes two different metabolic states; high glucose levels (glu > *alpha*) result in an ethanol yield of 0.372, and low glucose levels (glu $\leq$ *alpha*) result in an ethanol yield of 0.436. Remaining carbon is assumed to be allocated towards growth, occurring to a larger extent at high glucose levels according to the model. This is probably the reason why the flow rate is very low (0.1128 Lh^{-1}) during the continuous phase: the low biomass yield results in wash-out of cells if the flow rate is increased. Another possible explanation to the low flow rate chosen by the model could be that the randomly generated exponential relationship between ethanol concentration and refractive index is in reality not exponential. Obviously, this type of relationships must be experimentally determined in each specific media for the model to be accurate.

5.3 Future prospects

Experimental and computational analyses of xylose fermentation show that more research on C5/C6 fermenting strains is needed in order to understand the dynamic behaviour of glucose and xylose co-fermentation. In particular, the impact of ethanol on co-fermentation has barely been studied despite influencing several central metabolic pathways [56]. An investigation of transcriptional effects in cultures spiked with ethanol, before and after glucose consumption, would be of specific interest as this could indicate whether the effect of ethanol is related to transportation kinetics, central glycolytic pathways or general metabolic activity. Until further understanding of co-fermentation kinetics is revealed, there are however alternative methods available for increasing the rate of xylose fermentation. One approach could be to reduce the bottleneck of xylose uptake by increasing expression of hexose transporters that promote xylose uptake through reprogramming of gene transcription on a genomic scale. Using a method called *global Transcription Machinery Engineering* (gTME), mutations in the TATA-binding domain (*SP15*) of RNA polymerase II transcription factor D can be induced in order to modulate promoter specificity [57]. Random mutagenesis of *SP15* and a selective method such as adaptive laboratory evolution can be combined to obtain strains with favourable phenotypes such as increased xylose transmembrane transportation, without the requirement of prior knowledge about which genes should be targeted.

Modelling biological systems is a powerful tool to predict and understand complex microbial behaviour [58]. While physical demonstrations of fermentation technologies are expensive and time-consuming to perform, *in silico* fermentations can easily be adapted to costumer prerequisites without neither economical nor extensive time investments. Such simulations also hold great demonstrative value as variables are illustrated over time in each tank, providing information that is

easily grasped. Furthermore, in combination with existing expert integration systems for industrial fermentation plants [59], models of fermentation could be used to create an autonomous system that adjusts flowrate and biomass recirculation according to the current state of the fermentation.

Models presented in this report were constrained to a few external variables that are easily measured and to data extracted from batch cultures. There is great potential of improvement if data from continuous fermentations with hydrolysate as substrate are included in parameter optimization. Further development of kinetic expressions is also suggested as a future work, for example including a more dynamic differential equation for biomass and individual ethanol and biomass yields for glucose and xylose.

6 Conclusions

The increased fermentative rate of xylose observed by Sekab when ethanol was added initially could not be demonstrated in defined media with 20 gL^{-1} ethanol and equal amounts of glucose and xylose due to large deviations in replicates. However, each individual experiment showed a reduced fermentation rate during glucose consumption and an equal or increased fermentative rate during xylose consumption when 20 gL^{-1} ethanol was added initially. Furthermore, the maximum rate of xylose consumption was found equally fast regardless of glucose availability, although a $\sim$ 15 hour delay in xylose consumption onset occurred when glucose was absent. This indicates that the presence of glucose is not necessarily a decisive factor for xylose fermentation rate, but may facilitate cellular adaptation to utilization of xylose. Similarly, adding ethanol caused a delay in xylose consumption onset but did not reduce the maximum fermentative rate. The cellular mechanisms behind increased fermentative rate during the latter phase of co-fermentation remain uncertain, but findings presented in this report suggest that the effect of ethanol differs between glucose and xylose fermentation. A knowledge gap in the interplay between xylose metabolism and other fermentative substrates and products was highlighted, emphasizing the need for more in-depth research within this field. Although current understanding of regulatory mechanisms of xylose fermentation is insufficient to accurately model co-fermentations, a simulation of CoRyFee was developed based on simpler kinetics. This simulation holds large potential for Sekab as CoRyFee fermentations could be simulated with potential costumers' own substrate composition as input and be used to predict overall performance.

Acknowledgements

Working on site at Sekab in Örnsköldsvik has been a rewarding experience and I have gained a lot of valuable knowledge beyond the scope of this thesis. While leaving Chalmers after four and a half years feels strange I am very excited for what comes next. In February I will enter a new role as a development engineer and get to keep working with the talented and committed team I have gotten to know during the past few months. I would like to express my greatest gratitude to the talented and committed team at Sekab and everyone else who have supported me throughout this process. In particular, a massive thank you to:

- My supervisor and friend Dr. Adnan Cavka, development engineer at Sekab, who provided the basis for this project and has been an infinite source of motivation, ideas and knowledge from day one.
- Dr. Monica Normark, CTO at Sekab E-Technology AB, for giving me the opportunity to work with the innovative engineers at Sekab and for compassion and advice anytime needed.
- RISE Processum and MoRe research, for letting me use their laboratory facilities and equipment and their biotechnology group for making me feel very welcome in the lab and for always being ready to help out.
- Sekab consultant Elias Sundvall. His expertise in HPLC analysis has been invaluable for this project.
- PhD Jessica Sjöstedt at MoRe research for assisting with light microscopy.
- Fredrik Johansson for profound proofreading of this report and Jonas Wennermark for constant encouragement and advice on data analysis and visualization.

Mathilda Johansson
2022-01-01

References

1. Scripps Institution of Oceanography USD. The Keeling Curve. Available from: https://keelingcurve.ucsd.edu/. (accessed: 2021-11-03)
2. IPCC. Climate Change 2014: Impacts, Adaptation, and Vulnerability. Part A: Global and Sectoral Aspects. Contribution of Working Group II to the Fifth Assessment Report of the Intergovernmental Panel on Climate Change. Christopher B. Field, Vicente R. Barros, David Jon Dokken, Katharine J. Mach, Michael D. Mastrandrea, T. Eren Bilir, Monalisa Chatterjee, Kristie L. Ebi, Yuka Otsuki Estrada, Robert C. Genova, Betelhem Girma, Eric S. Kissel, Andrew N. Levy, Sandy MacCracken, Patricia R. Mastrandrea, Leslie L. White. 2014
3. Hannah Ritchie and Max Roser. Our World in Data: CO2 and Greenhouse Gas Emissions. 2020. Available from: https://ourworldindata.org/emissions-by-sector. accessed: 2021-11-23
4. Swedish Energy Agency. Greenhouse gas reduction mandate. 2020. Available from: http://www.energimyndigheten.se/en/sustainability/sustainable-fuels/greenhouse-gas-reduction-mandate/. accessed 2021-11-03
5. SFS 2021:747. *Lag om reduktion av växthusgasutsläpp från vissa fossila drivmedel*. Available from: https://rkrattsbaser.gov.se/sfst?bet=2017:1201
6. biofuel. 2021 Sep. Available from: https://www.britannica.com/technology/biofuel. accessed: 2021-11-18
7. Niphadkar S, Bagade P, and Ahmed S. Bioethanol production: insight into past, present and future perspectives. Biofuels 2018; 9:229–38
8. Swedish forest industries. Facts & Figures: Sweden's forest industry in brief. Available from: https://www.forestindustries.se/forest-industry/facts-and-figures/. accessed: 2021-11-23
9. The World Bank. Forest area (% of land area) - Sweden. 2020. Available from: https://data.worldbank.org/indicator/AG.LND.FRST.ZS?locations=SE
10. Naturvårdsverket. Tillväxt och avverkningar i skogen. 2022. Available from: https://www.naturvardsverket.se/data-och-statistik/skog/skog-tillvaxt-och-avverkningar/. Accessed: 2022-01-10
11. SEKAB. Our history. Available from: https://www.sekab.com/en/about-us/about-the-company/our-history/. accessed: 2021-11-03
12. Pettersen RC. The chemical composition of wood. The chemistry of solid wood 1984; 207:57–126
13. Azhar SHM, Abdulla R, Jambo SA, Marbawi H, Gansau JA, Faik AAM, and Rodrigues KF. Yeasts in sustainable bioethanol production: A review. Biochemistry and Biophysics Reports 2017; 10:52–61
14. Talebnia F, Karakashev D, and Angelidaki I. Production of bioethanol from wheat straw: an overview on pretreatment, hydrolysis and fermentation. Bioresource technology 2010; 101:4744–53
15. Chen H and Qiu W. Key technologies for bioethanol production from lignocellulose. Biotechnology Advances 2010; 28:556–62

16. SEKAB. Our process. B. Available from: https://www.sekab.com/en/this-is-how-it-works/biorefinery-demo-plant/our-process/. accessed: 2021-11-04
17. Brethauer S and Wyman CE. Continuous hydrolysis and fermentation for cellulosic ethanol production. Bioresource technology 2010; 101:4862–74
18. Knudsen JD and Rønnow B. Extended fed-batch fermentation of a C5/C6 optimised yeast strain on wheat straw hydrolysate using an online refractive index sensor to measure the relative fermentation rate. Scientific reports 2020; 10:1–9
19. Subtil T and Boles E. Competition between pentoses and glucose during uptake and catabolism in recombinant Saccharomyces cerevisiae. Biotechnology for Biofuels 2012; 5:1–12
20. Pfeiffer T and Morley A. An evolutionary perspective on the Crabtree effect. Frontiers in molecular biosciences 2014; 1:17
21. Zimmermann FK and Entian KD. Yeast sugar metabolism. CRC Press, 1997
22. De Deken R. The Crabtree effect: a regulatory system in yeast. Microbiology 1966; 44:149–56
23. Wenger JW, Schwartz K, and Sherlock G. Bulk segregant analysis by high-throughput sequencing reveals a novel xylose utilization gene from Saccharomyces cerevisiae. PLoS genetics 2010; 6:e1000942
24. Kötter P, Amore R, Hollenberg CP, and Ciriacy M. Isolation and characterization of the Pichia stipitis xylitol dehydrogenase gene, XYL2, and construction of a xylose-utilizing Saccharomyces cerevisiae transformant. Current genetics 1990; 18:493–500
25. Kuyper M, Harhangi HR, Stave AK, Winkler AA, Jetten MS, Laat WT de, Ridder JJ den, Op den Camp HJ, Dijken JP van, and Pronk JT. High-level functional expression of a fungal xylose isomerase: the key to efficient ethanolic fermentation of xylose by Saccharomyces cerevisiae? FEMS yeast research 2003; 4:69–78
26. Karhumaa K, Sanchez RG, Hahn-Hägerdal B, and Gorwa-Grauslund MF. Comparison of the xylose reductase-xylitol dehydrogenase and the xylose isomerase pathways for xylose fermentation by recombinant Saccharomyces cerevisiae. Microbial cell factories 2007; 6:1–10
27. Young E, Lee SM, and Alper H. Optimizing pentose utilization in yeast: the need for novel tools and approaches. Biotechnology for biofuels 2010; 3:1–12
28. Nissen TL, Anderlund M, Nielsen J, Villadsen J, and Kielland-Brandt MC. Expression of a cytoplasmic transhydrogenase in Saccharomyces cerevisiae results in formation of 2-oxoglutarate due to depletion of the NADPH pool. Yeast 2001; 18:19–32
29. Goncalves DL, Matsushika A, Belisa B, Goshima T, Bon EP, and Stambuk BU. Xylose and xylose/glucose co-fermentation by recombinant Saccharomyces cerevisiae strains expressing individual hexose transporters. Enzyme and microbial technology 2014; 63:13–20
30. Horák J. Regulations of sugar transporters: insights from yeast. Current genetics 2013; 59:1–31
31. Saloheimo A, Rauta J, Stasyk V, Sibirny AA, Penttilä M, and Ruohonen L. Xylose transport studies with xylose-utilizing Saccharomyces cerevisiae strains expressing heterologous and homologous permeases. Applied microbiology and biotechnology 2007; 74:1041–52
32. Runquist D, Fonseca C, Rådström P, Spencer-Martins I, and Hahn-Hägerdal B. Expression of the Gxf1 transporter from Candida intermedia improves fermentation performance in recom-

binant xylose-utilizing Saccharomyces cerevisiae. Applied microbiology and biotechnology 2009; 82:123–30
33. Salusjärvi L, Pitkänen JP, Aristidou A, Ruohonen L, and Penttilä M. Transcription analysis of recombinant Saccharomyces cerevisiae reveals novel responses to xylose. Applied biochemistry and biotechnology 2006; 128:237–73
34. Salusjärvi L, Kankainen M, Soliymani R, Pitkänen JP, Penttilä M, and Ruohonen L. Regulation of xylose metabolism in recombinant Saccharomyces cerevisiae. Microbial cell factories 2008; 7:1–16
35. Kayikci Ö and Nielsen J. Glucose repression in Saccharomyces cerevisiae. FEMS yeast research 2015; 15:fov068
36. Wu M, Li H, Wei S, Wu H, Wu X, Bao X, Hou J, Liu W, and Shen Y. Simulating extracellular glucose signals enhances xylose metabolism in recombinant Saccharomyces cerevisiae. Microorganisms 2020; 8:100
37. Briggs GE and Haldane JBS. A note on the kinetics of enzyme action. Biochemical journal 1925; 19:338
38. Ainsworth S. Michaelis-menten kinetics. *Steady-state enzyme kinetics*. Springer, 1977 :43–73
39. Nosrati-Ghods N, Harrison ST, Isafiade AJ, and Leng Tai S. Mathematical Modelling of Bioethanol Fermentation From Glucose, Xylose or Their Combination–A Review. ChemBioEng Reviews 2020; 7:68–88
40. Levenspiel O. The Monod equation: a revisit and a generalization to product inhibition situations. Biotechnology and bioengineering 1980; 22:1671–87
41. Luong J. Kinetics of ethanol inhibition in alcohol fermentation. Biotechnology and bioengineering 1985; 27:280–5
42. Alff-Tuomala S, Salusjärvi L, Barth D, Oja M, Penttilä M, Pitkänen JP, Ruohonen L, and Jouhten P. Xylose-induced dynamic effects on metabolism and gene expression in engineered Saccharomyces cerevisiae in anaerobic glucose-xylose cultures. Applied microbiology and biotechnology 2016; 100:969–85
43. Sulieman AK, Putra MD, Abasaeed AE, Gaily MH, Al-Zahrani SM, and Zeinelabdeen MA. Kinetic modeling of the simultaneous production of ethanol and fructose by Saccharomyces cerevisiae. Electronic Journal of Biotechnology 2018; 34:1–8
44. SEKAB. CoRyFee. C. Available from: `https://www.sekab.com/en/products-services/product/project-coryfee/`. accessed: 2022-01-08
45. Biotechnology Information NC for. PubChem Compound Summary for CID 962, Water. 2022. Available from: `https://pubchem.ncbi.nlm.nih.gov/compound/Water`. Accessed: 2022-01-08
46. Mat Yunus WM bin and Abdul Rahman A bin. Refractive index of solutions at high concentrations. Applied optics 1988; 27:3341–3
47. Dongare M, Buchade P, and Shaligram A. Refractive index based optical Brix measurement technique with equilateral angle prism for sugar and Allied Industries. Optik 2015; 126:2383–5
48. Magwaza LS and Opara UL. Analytical methods for determination of sugars and sweetness of horticultural products—A review. Scientia Horticulturae 2015; 184:179–92

49. Morrill K, Polo J, Lago A, Campbell J, Quigley J, and Tyler H. Estimate of serum immunoglobulin G concentration using refractometry with or without caprylic acid fractionation. Journal of dairy science 2013; 96:4535–41
50. Nyau V, Mwanza E, and Moonga H. Physico-chemical qualities of honey harvested from different beehive types in Zambia. African Journal of Food, Agriculture, nutrition and development 2013; 13
51. Von Stockar U and Liu JS. Does microbial life always feed on negative entropy? Thermodynamic analysis of microbial growth. Biochimica et Biophysica Acta (BBA)-Bioenergetics 1999; 1412:191–211
52. Kuyper M, Winkler AA, Dijken JP van, and Pronk JT. Minimal metabolic engineering of Saccharomyces cerevisiae for efficient anaerobic xylose fermentation: a proof of principle. FEMS yeast research 2004; 4:655–64
53. Westman JO and Franzén CJ. Current progress in high cell density yeast bioprocesses for bioethanol production. Biotechnology journal 2015; 10:1185–95
54. Sohn SB, Kim TY, Lee JH, and Lee SY. Genome-scale metabolic model of the fission yeast Schizosaccharomyces pombe and the reconciliation of in silico/in vivo mutant growth. BMC systems biology 2012; 6:1–12
55. Özcan S, Dover J, and Johnston M. Glucose sensing and signaling by two glucose receptors in the yeast Saccharomyces cerevisiae. The EMBO journal 1998; 17:2566–73
56. Stanley D, Bandara A, Fraser S, Chambers P, and Stanley GA. The ethanol stress response and ethanol tolerance of Saccharomyces cerevisiae. Journal of applied microbiology 2010; 109:13–24
57. Alper H, Moxley J, Nevoigt E, Fink GR, and Stephanopoulos G. Engineering yeast transcription machinery for improved ethanol tolerance and production. Science 2006; 314:1565–8
58. Lopatkin AJ and Collins JJ. Predictive biology: modelling, understanding and harnessing microbial complexity. Nature Reviews Microbiology 2020; 18:507–20
59. Guerreiro MA, Andrietta SR, and Maugeri F. Expert system for the design of an industrial fermentation plant for the production of alcohol. Journal of Chemical Technology & Biotechnology: International Research in Process, Environmental AND Clean Technology 1997; 68:163–70

Supplementary material

Error estimation of CO_2 loss measurements

100 mL cultivation flasks with 25 mL water and varying ethanol concentrations were incubated in 30 °C with 140 rpm agitation during eight hours with regular weight measurements, as shown in Figure S17. The initial weight gain of the 20 gL^{-1} ethanol sample is presumably due to the fast evaporation of a liquid droplet spilled on the outside of the flask during preparation. To compensate for this error when estimating mean weight loss and standard deviation, the second measurement is used as initial weight. Since cultivation flasks were incubated for 30 minutes prior to addition of ethanol and sampling, this error is not expected to occur in the experimental data.

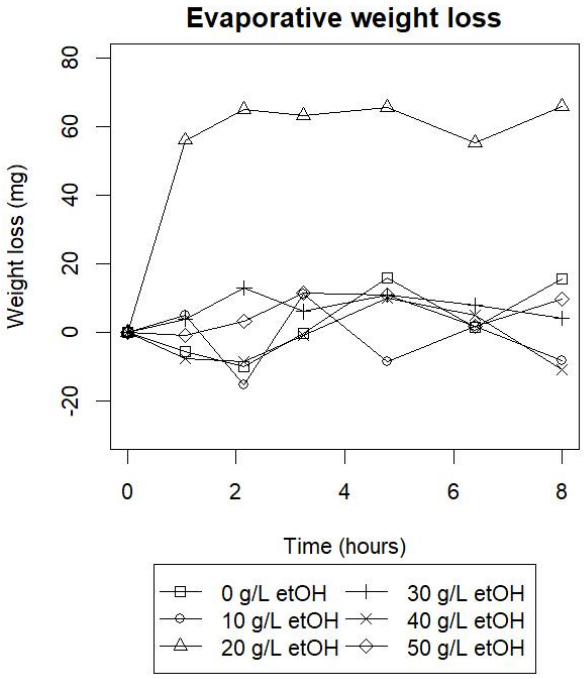

Figure S17: Estimation of evaporative weight loss. Cultivations with water and a range of ethanol concentrations were inclubated for 8 hours and the weight loss was monitored.

The mean weight loss over 8 hours for all samples was determined to 2.49 mg, corresponding to less than 1% of the total weight loss in the experiments presented in this study. The average standard deviation between and within the samples was calculated to 7.59.

Calculation of nitrogen assimilation and biomass formation from proton release

Before incubation:

$$pH = 5.60$$
$$[H^+_{free}] = 10^{-5.6}/0.75 = 3.3492 * 10^{-6} mol/L$$
$$[N_{consumed}] = [H^+_{free}]/4 = 8.3730 * 10^{-7} mol/L$$
$$[Biomass] = [N_{consumed}]/0.08 = 1.0466 * 10^{-5} mol/L$$
$$= 1.0466 * 10^{-5} * 319 = 3.339 * 10^3 g = 3.3 mgL^{-1}$$

After 5 hours incubation, no added ethanol:

$$pH = 4.01$$
$$[H^+_{free}] = 10^{-4.01}/0.75 = 1.3030 * 10^{-4} mol/L$$
$$[N_{consumed}] = [H^+_{free}]/4 = 3.2575 * 10^{-5} mol/L$$
$$[Biomass] = [N_{consumed}]/0.08 = 4.0719 * 10^{-4} mol/L$$
$$= 4.0719 * 10^{-4} * 319 = 0.1300 g = 130.0 mgL^{-1}$$
$$[\Delta biomass] = 130.0 - 3.3 = 126.7 mgL^{-1}$$

After 5 hours incubation, 20 gL^{-1} added ethanol:

$$pH = 4.24$$
$$[H^+_{free}] = 10^{-4.24}/0.75 = 7.6725 * 10^{-5} mol/L$$
$$[N_{consumed}] = [H^+_{free}]/4 = 1.9181 * 10^{-5} mol/L$$
$$[Biomass] = [N_{consumed}]/0.08 = 2.3978 * 10^{-4} mol/L$$
$$= 2.3978 * 10^{-4} * 319 = 0.07649 g = 76.5 mgL^{-1}$$
$$[\Delta biomass] = 76.5 - 3.3 = 73.2 mgL^{-1}$$

Computational model parameters

Without ethanol

Model based on Taumala et al. 2016

Parameter	Value	Unit
$v_{max,1}$	0.5821	$gg^{-1}g^{-1}$
$v_{max,2}$	0.1473	$gg^{-1}g^{-1}$
$K1$	2.0057	gL^{-1}
$K2$	0.3988	gL^{-1}
K_{glu}	1.4577	gL^{-1}
tau	3.7610	h
$Y_{es,1}$	0.3791	gg^{-1}
$Y_{es,2}$	0.4665	gg^{-1}
$alpha$	1.7282	gL^{-1}

Table 6: Optimized parameter values for kinetic model without ethanol inhibition.

With inhibition

Model based on Luong et al. 1985

Parameter	Value	Unit
E_{max}	85.7468	gL^{-1}
tau	3.2706	h
$alpha$	2.3033	gL^{-1}
K_{glu}	0.2006	gL^{-1}
a	1.2957	No unit
$Y_{es,1}$	0.3715	gg^{-1}
$Y_{es,2}$	0.4361	gg^{-1}
$v_{max,1}$	0.6171	$gg^{-1}g^{-1}$
$K1$	2.9270	gL^{-1}
$v_{max,2}$	0.2310	$gg^{-1}g^{-1}$
$K2$	0.4600	gL^{-1}

Table 7: Optimized parameter values för kinetic model with ethanol inhibition.

Defined media composition

Component	Concentration in media
Yeast Nitrogen Base w/o amino acids	6.7 gL^{-1}
Ammonium sulphate	5 gL^{-1}
Succinic acid (pH buffering)	5.9 gL^{-1}
KOH	Added until pH = 5.6
Glucose	25 gL^{-1}
Xylose	10, 25 or 50 gL^{-1}
Ethanol	0, 10, 20 or 40 gL^{-1}
milliQ water	Fill up to final volume

Table S8: Components in fermentation media and corresponding amounts.